Magnetic Reconnection Experiments on the MAGPIE Pulsed Power Generator

Jack W. D. Halliday (jack.halliday12@imperial.ac.uk)

L. G. Suttle (1), J. D. Hare (2), S. V. Lebedev (1), A. Ciardi (3), N. Loureiro (4), G. C. Burdiak (5), J. P. Chittenden (1), T. Clayson (5), T. Lane (6), D. Russell (1), E. R. Tubman (1) V. Valenzuela Villaseca (1)

(1) Imperial College London; (2) Max-Planck Institute for Plasma Physics, Munich; (3) Sorbonne University and Paris Observatory; (4) Massachusetts Institute of Technology; (5) First Light Fusion Ltd, Oxfordshire

Imperial College London

Multi-university Center for Pulsed-Power Driven High Energy Density Science

MAGPIE

Supported by EPSRC Grant No. EP/N013379/1, and by the US DOE Awards No. DE-F03-02NA00057, DE-SC-0001063, and DE-NA-0003764.

Structure of the reconnection layer

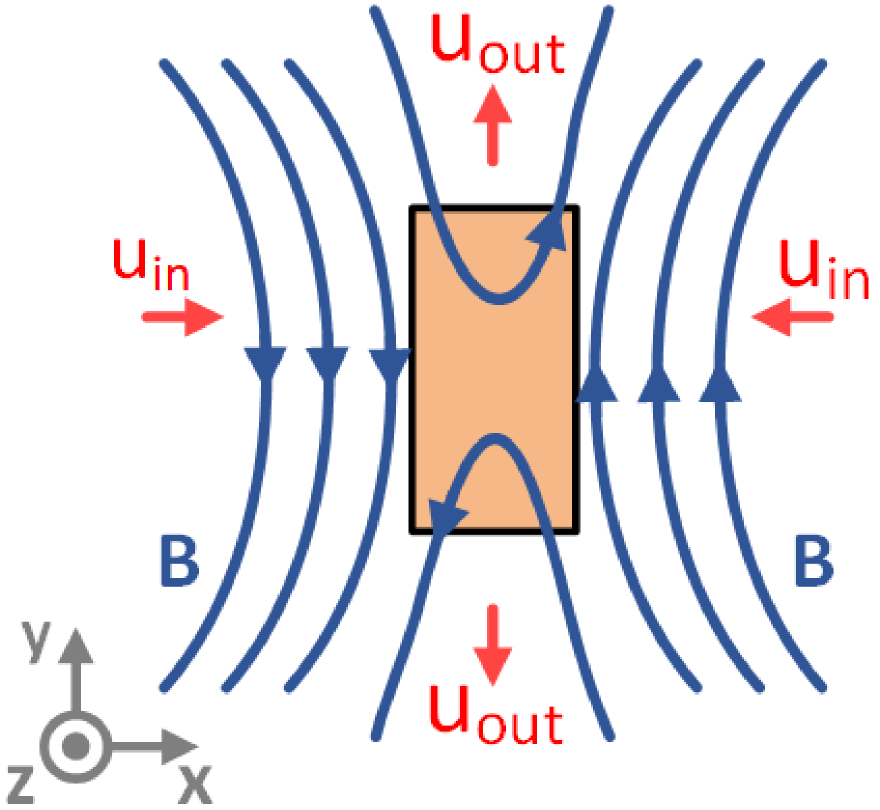

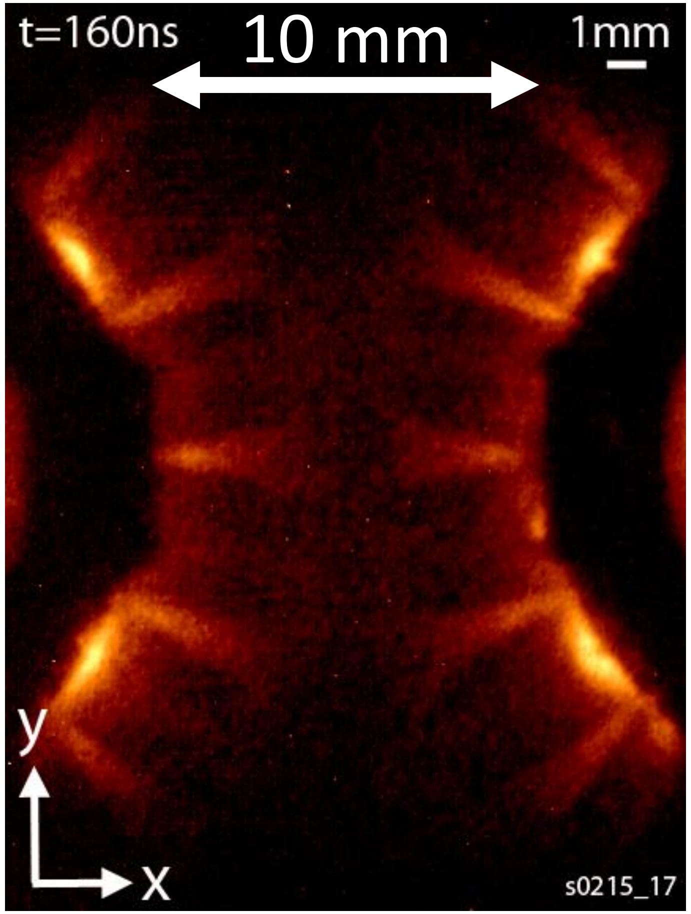

Overview

- Description of experimental setup
- Diagnostic techniques (Interferometry, Faraday Rotation Thomson Scattering)
- Demonstration of power balance
- Plasmoid unstable reconnection

The MAGPIE Current Generator

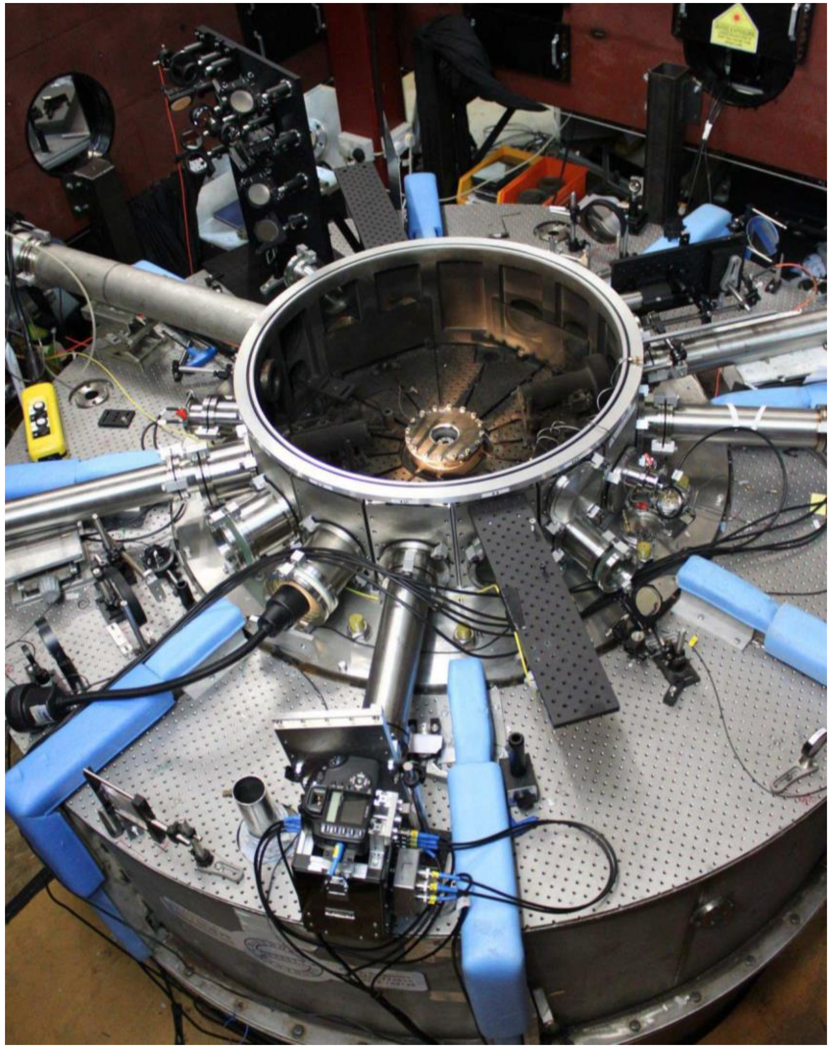

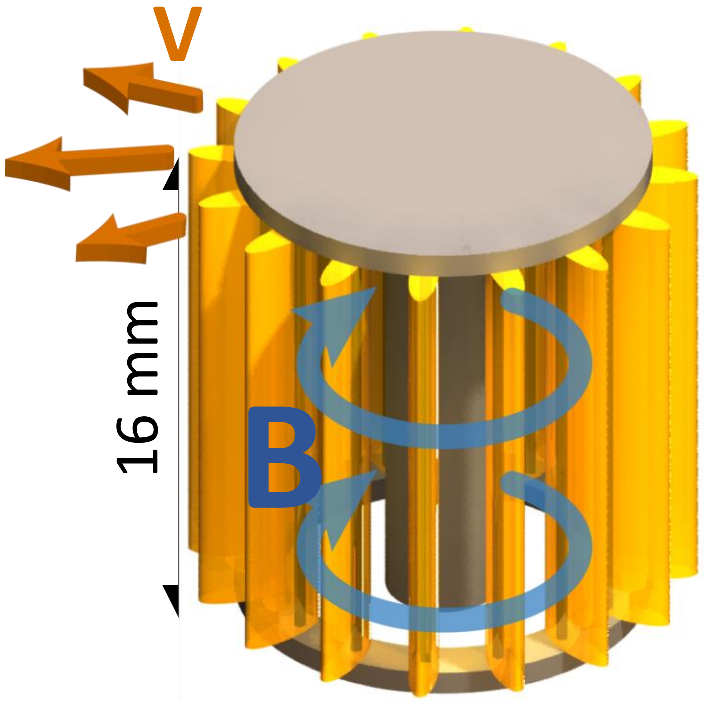

$T_{drive} \sim 500\,\mathrm{ns}$ $\quad I_{peak} \sim 1\ \mathrm{MA}$

The MAGPIE Current Generator

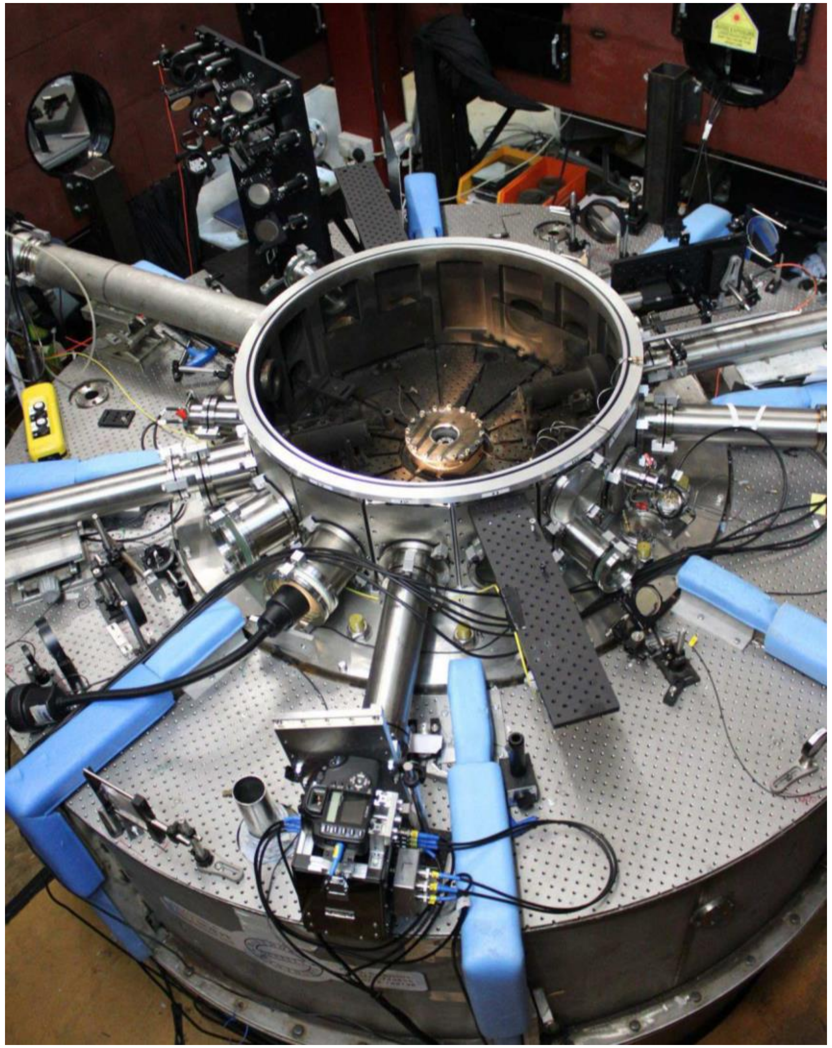

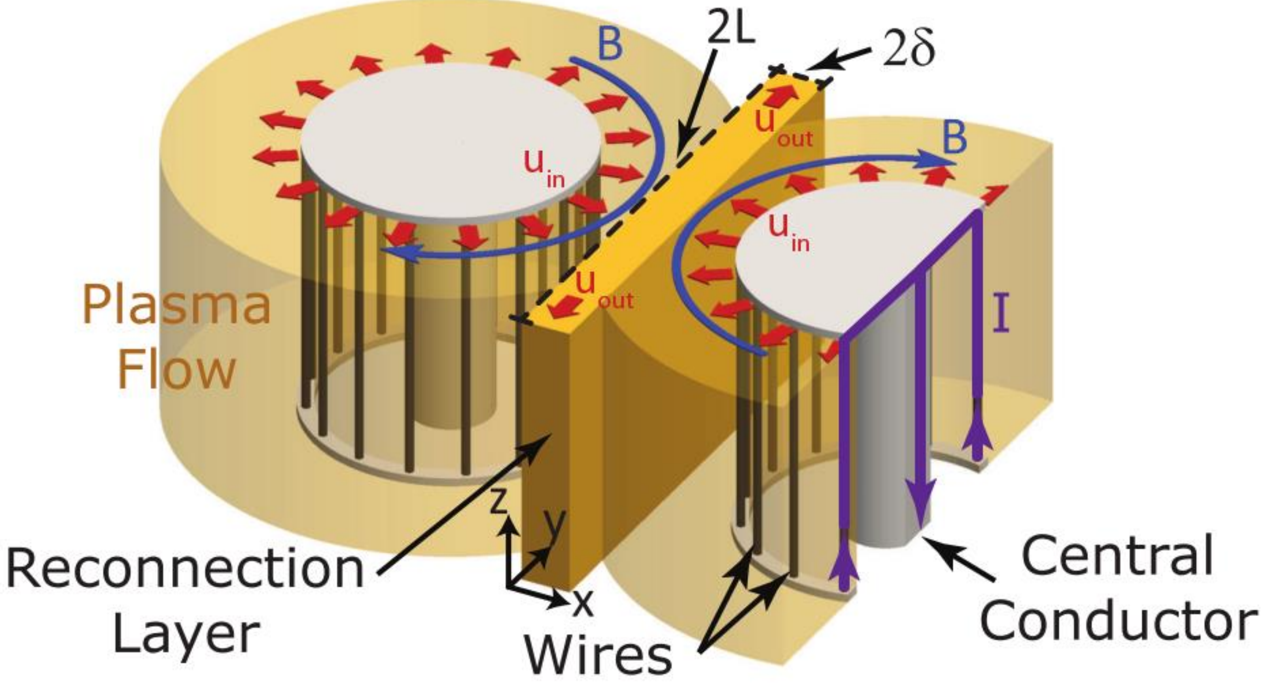

The MAGPIE Reconnection Framework

Parameter	Value
n_e	$\sim 10^{17-18}\ cm^{-3}$
B_{in}	$2 - 3\ T$
L	$\sim 10\ mm$
λ_{ei}	$\sim 0.1\ mm$

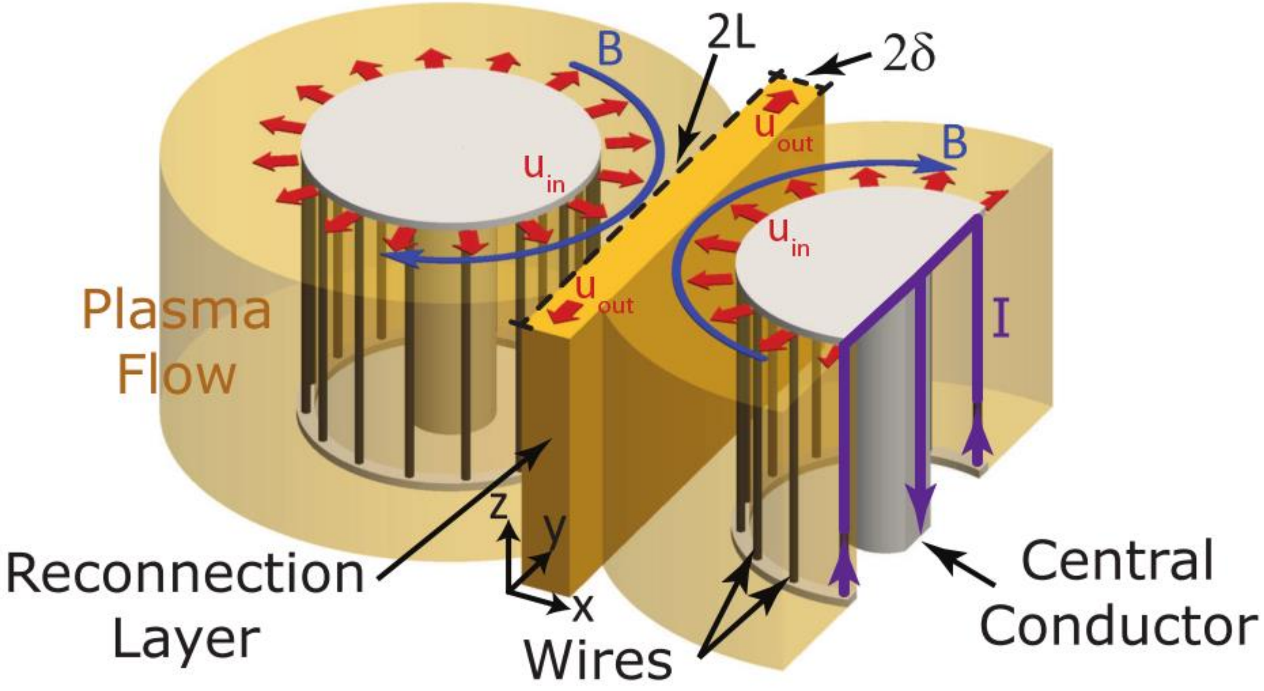

L. G. Suttle *et al.* – PRL 2016; PoP 2018

J. D. Hare *et al.* – PRL 2017; PoP 2017; PoP 2018

The MAGPIE Reconnection Framework

Carbon Plasma:

Sub-Alfvénic

Negligible radiation

$M_A = 0.7$

$\beta_{dyn} \sim 1$

$S \sim 100$

J.D. Hare *et al*. PRL (2017) , PoP (2017)

Aluminium Plasma:

Super-Alfvénic

Radiatively cooled

$M_A = 2.5$

$\beta_{dyn} \sim 10$

$S \sim 10$

L. Suttle *et al*. PRL (2016), PoP (2018)

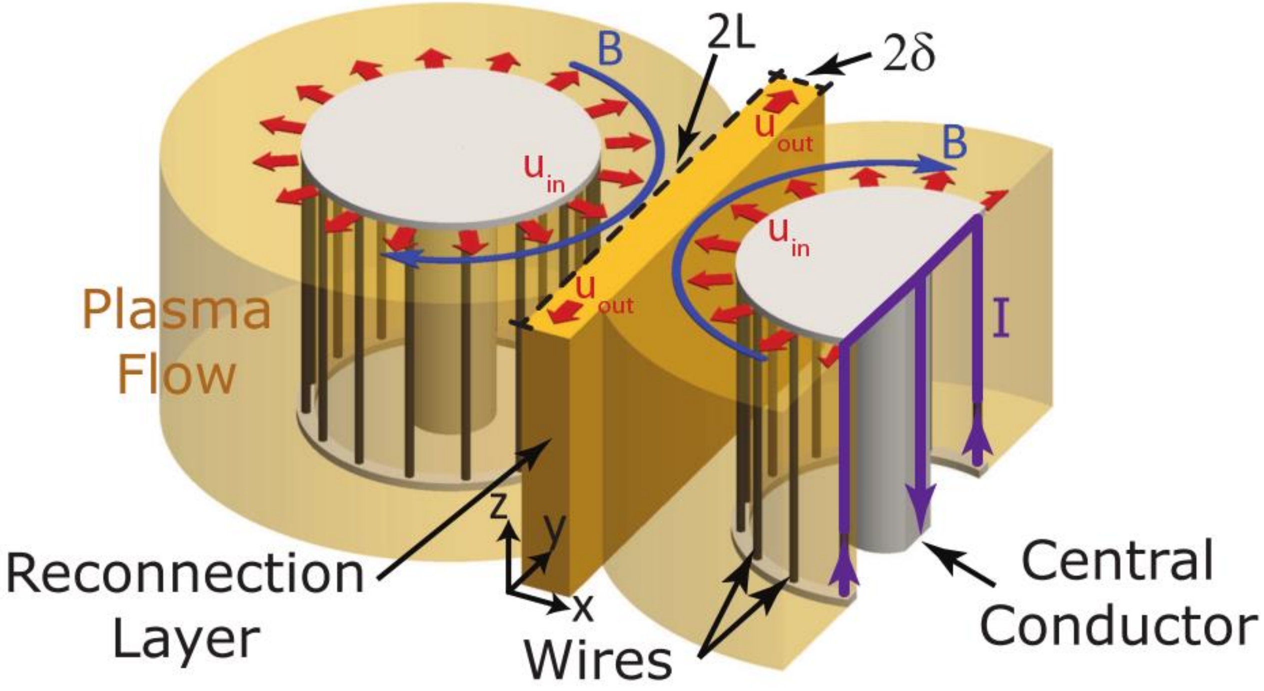

Comparison Paper: J. D. Hare *et al* PoP 2018

Overview

- Description of experimental setup
- Diagnostic techniques (Interferometry, Faraday Rotation Thomson Scattering)
- Demonstration of power balance
- Plasmoid unstable reconnection

Structure of the reconnection layer

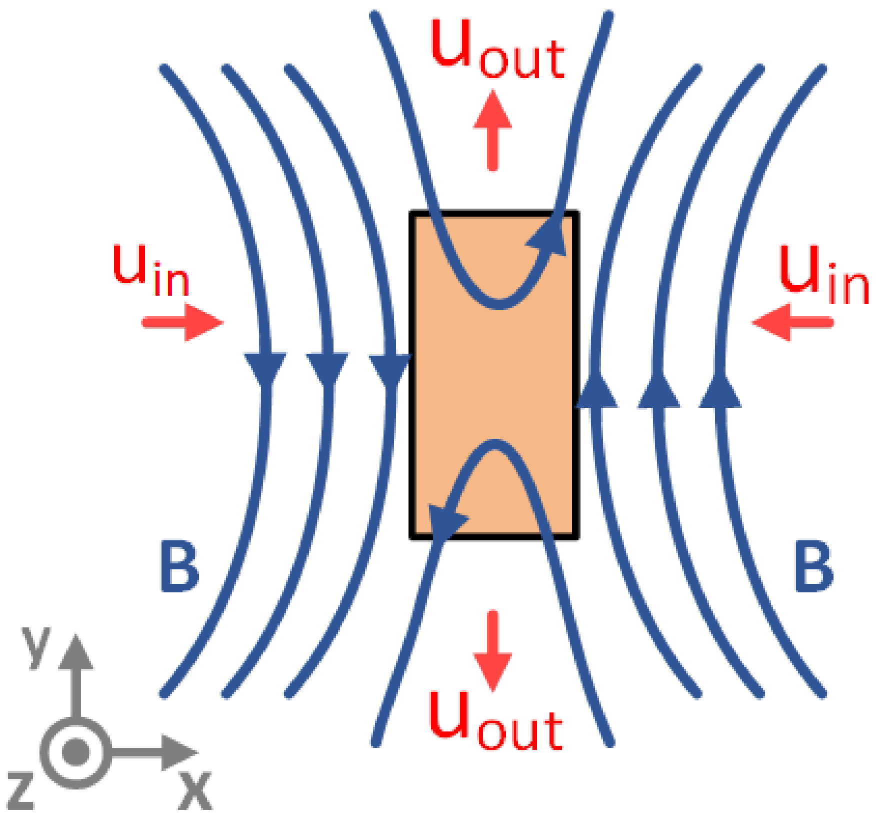

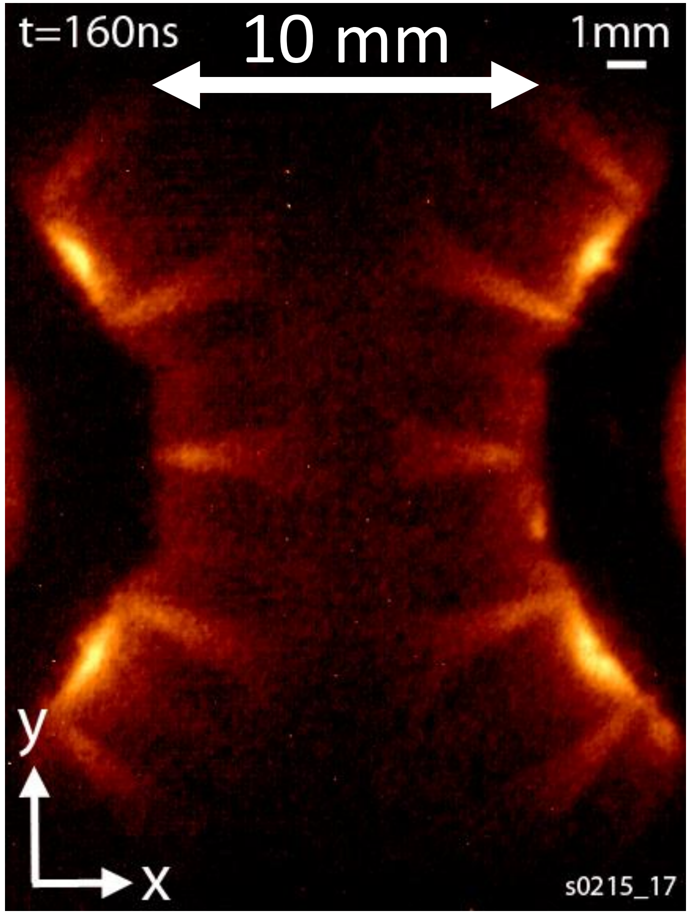

Structure of the reconnection layer

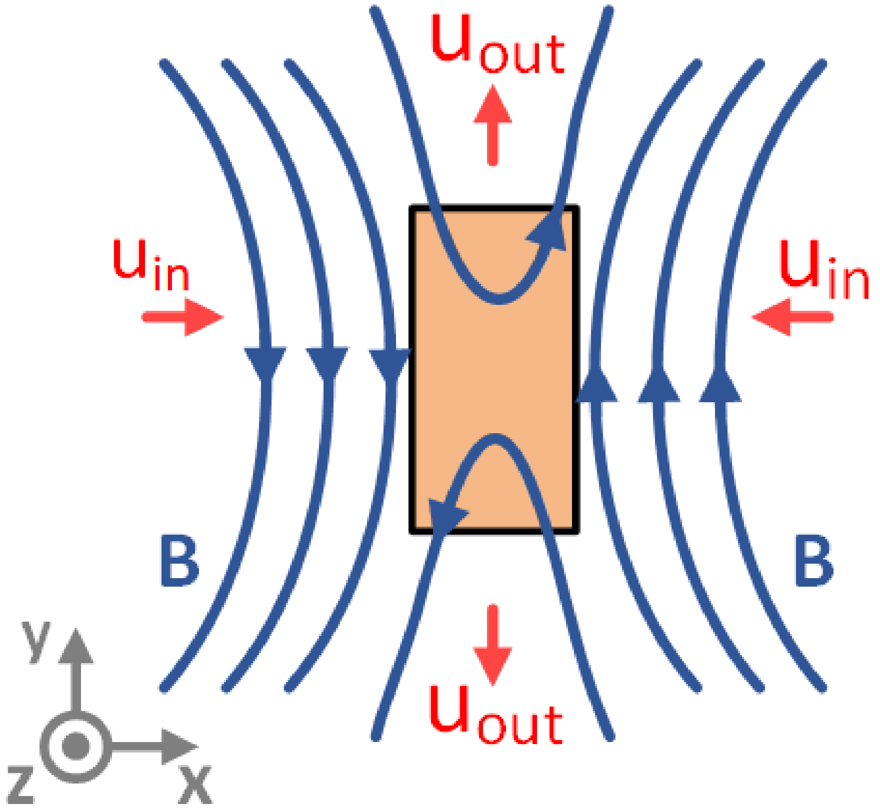

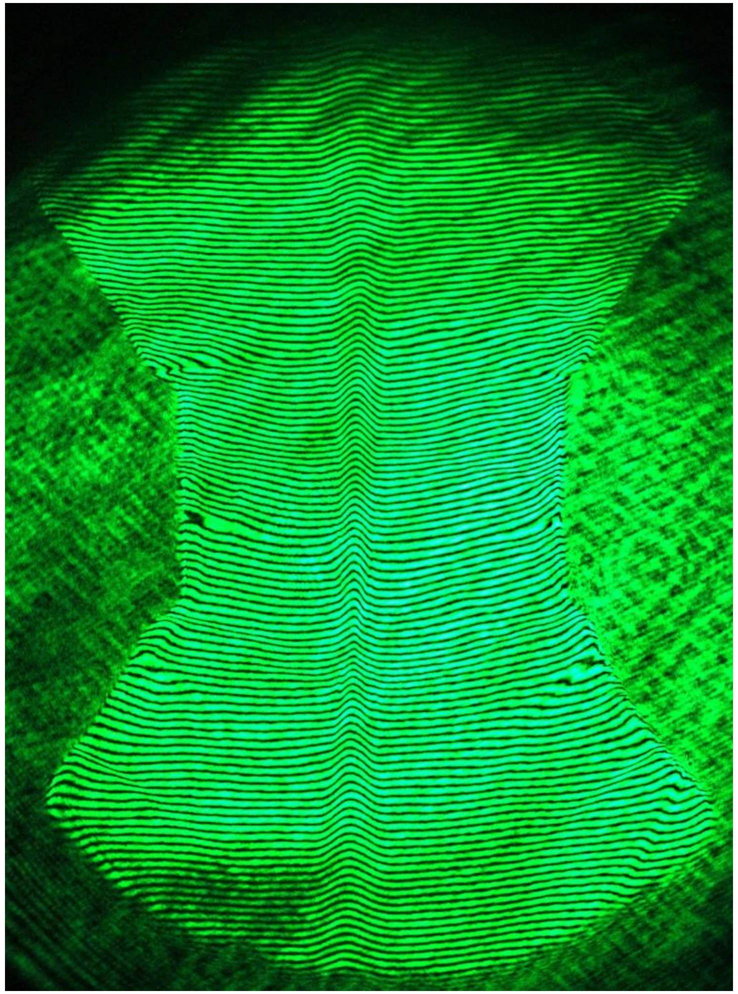

Structure of the reconnection layer

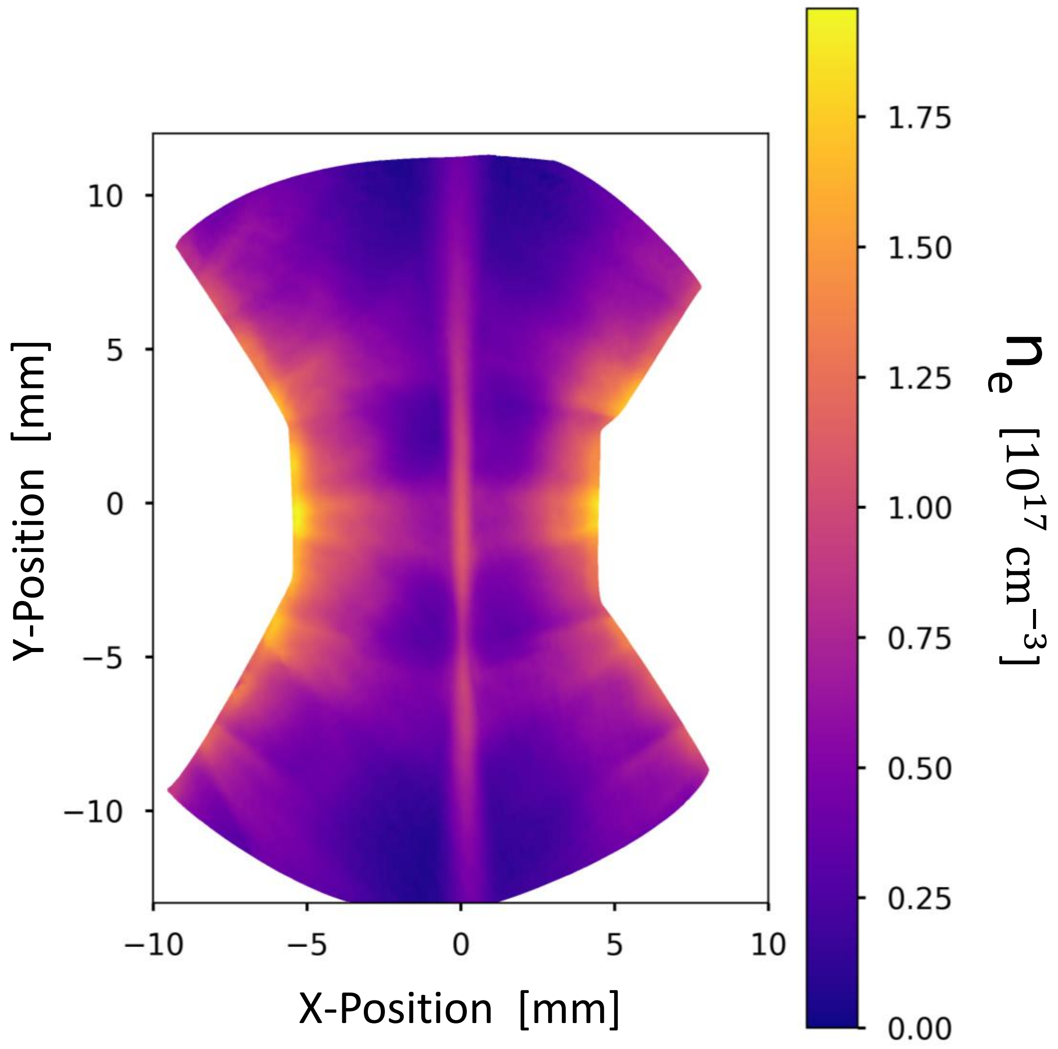

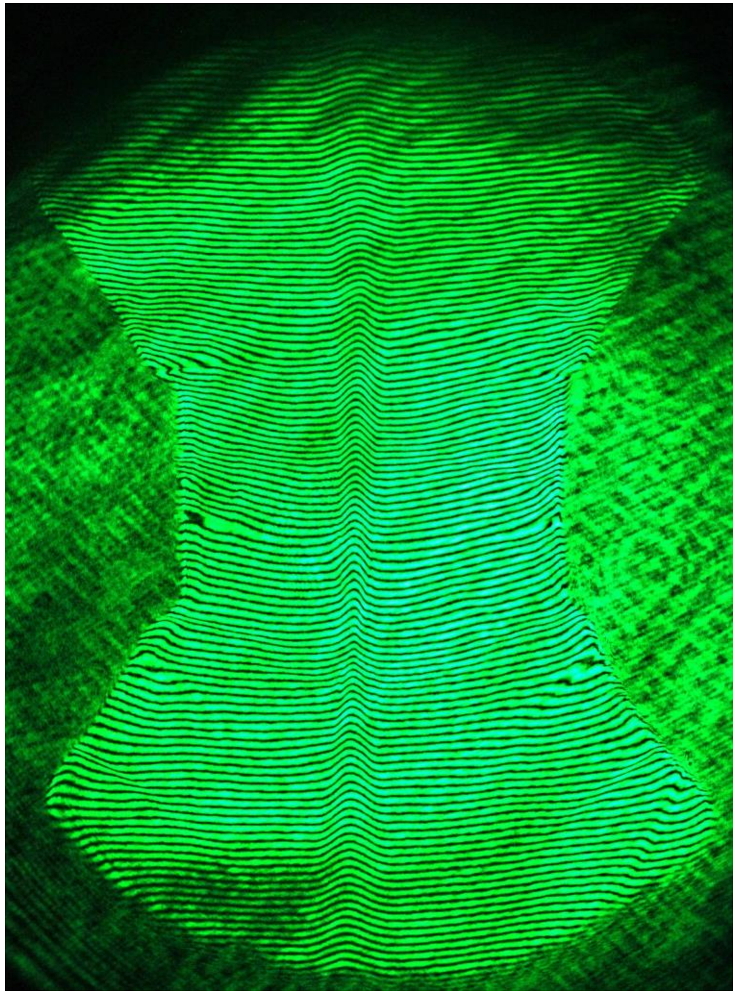

Magnetic Field Profile – Faraday Rotation

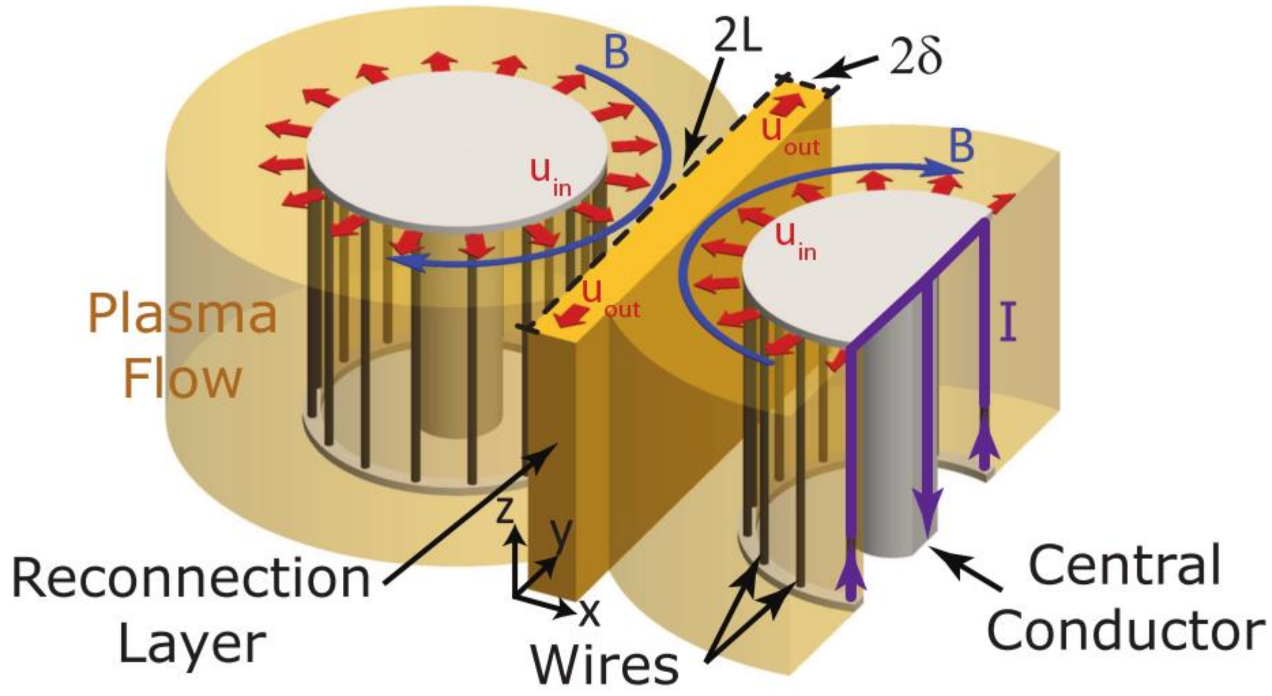

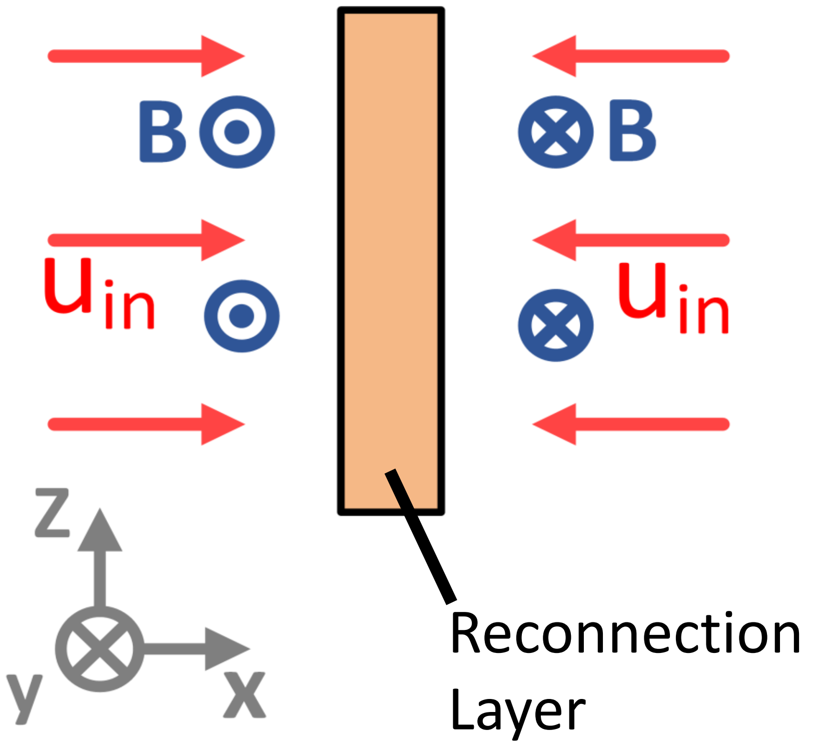

Magnetic Field Profile – Faraday Rotation

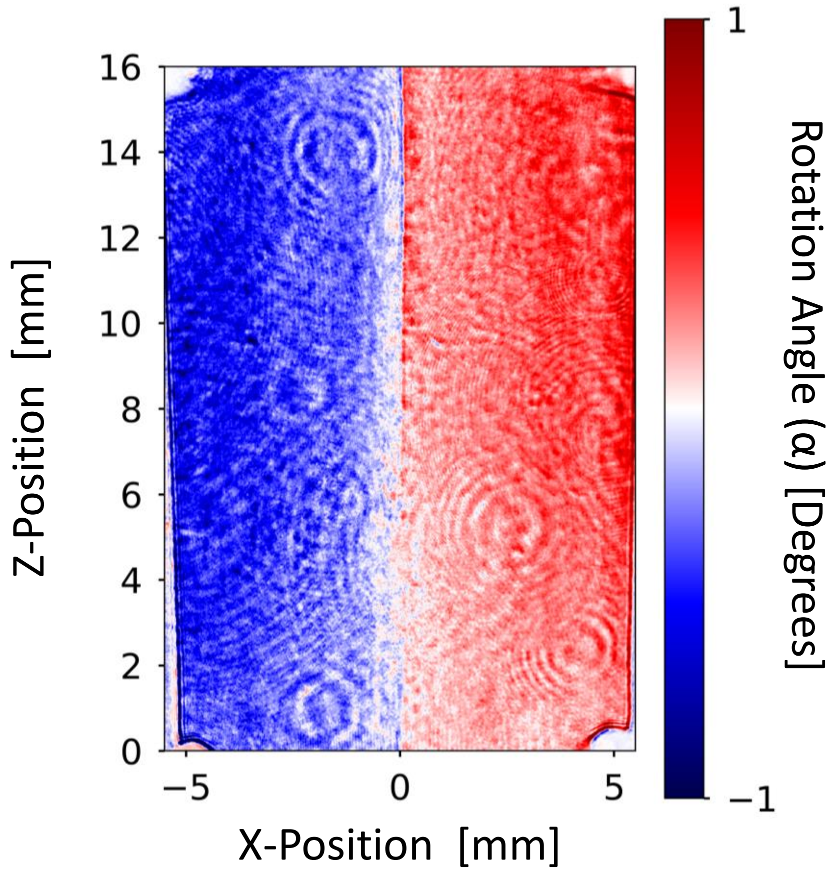

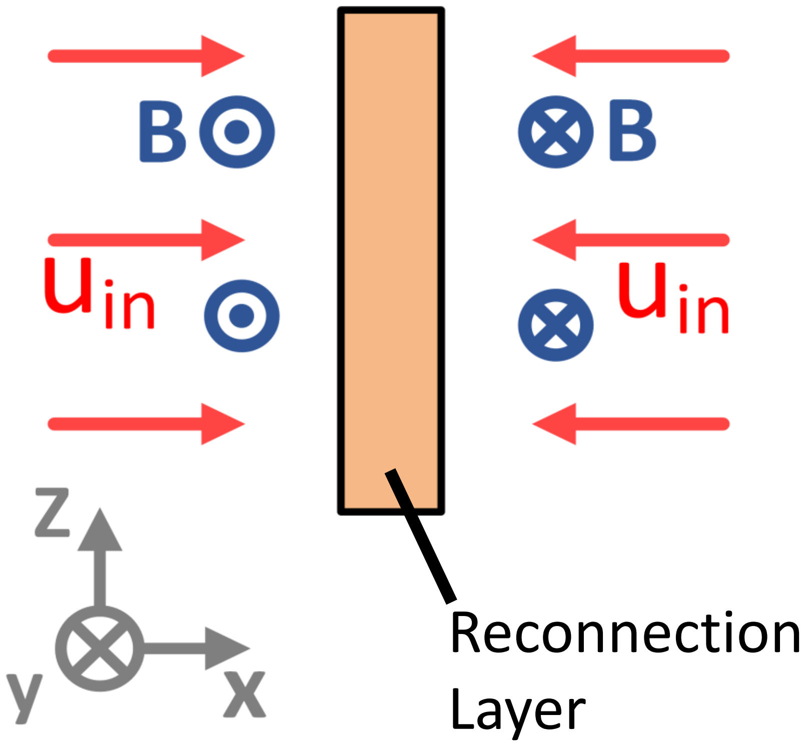

$$\alpha(x,z) \propto \int n_e B_y dy$$

Magnetic Field Profile – Faraday Rotation

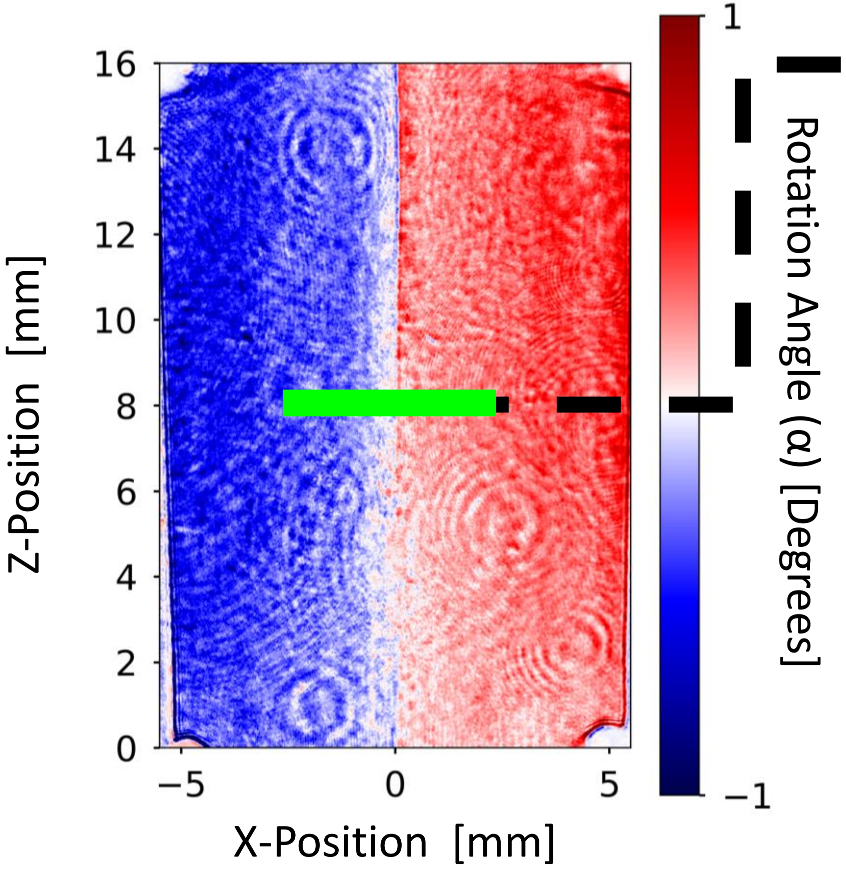

Carbon Plasma ($M_A < 1$)

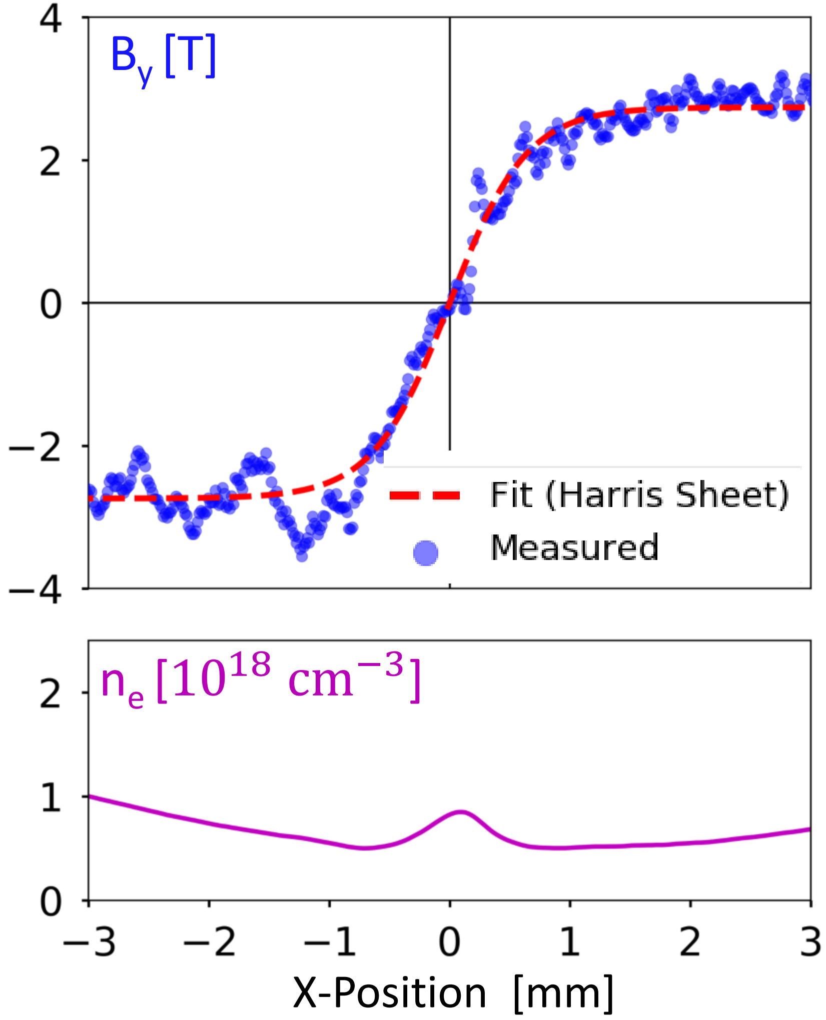

Magnetic Field Profile – Faraday Rotation

Aluminium Plasma ($M_A > 1$)

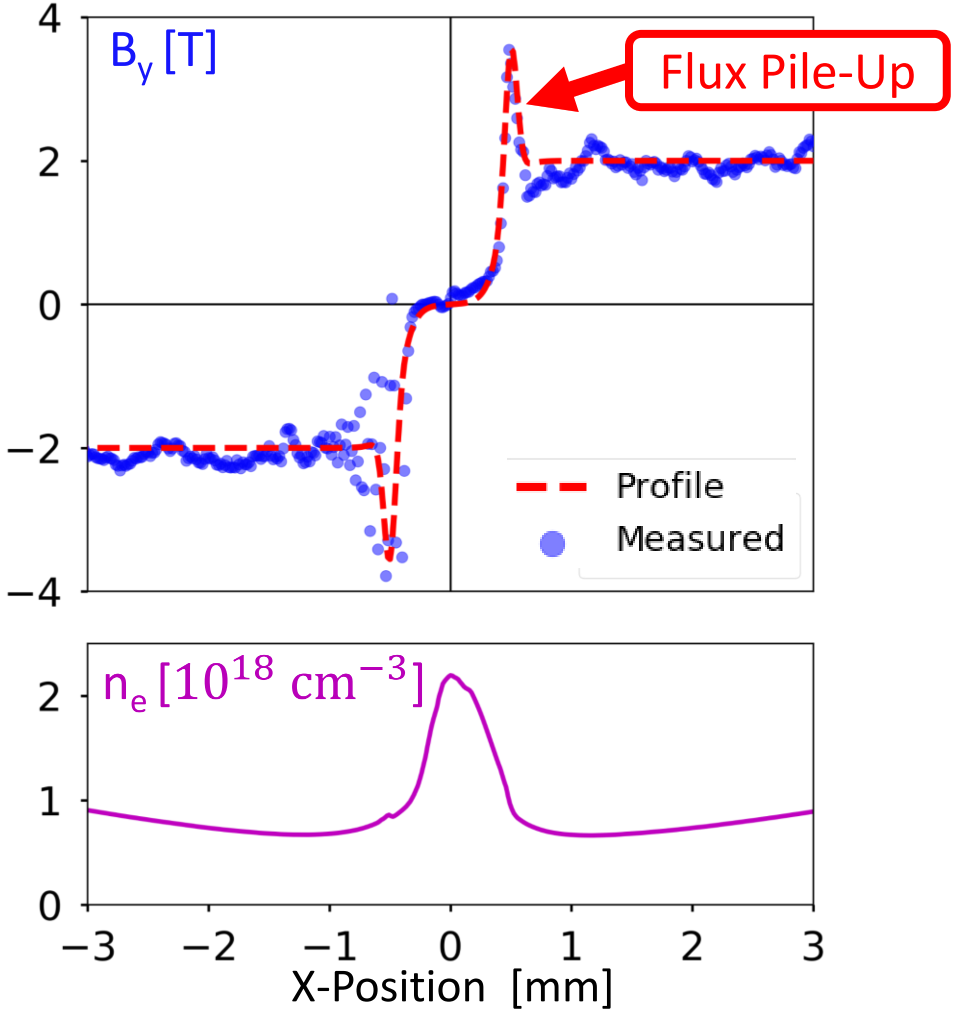

Carbon Plasma ($M_A < 1$)

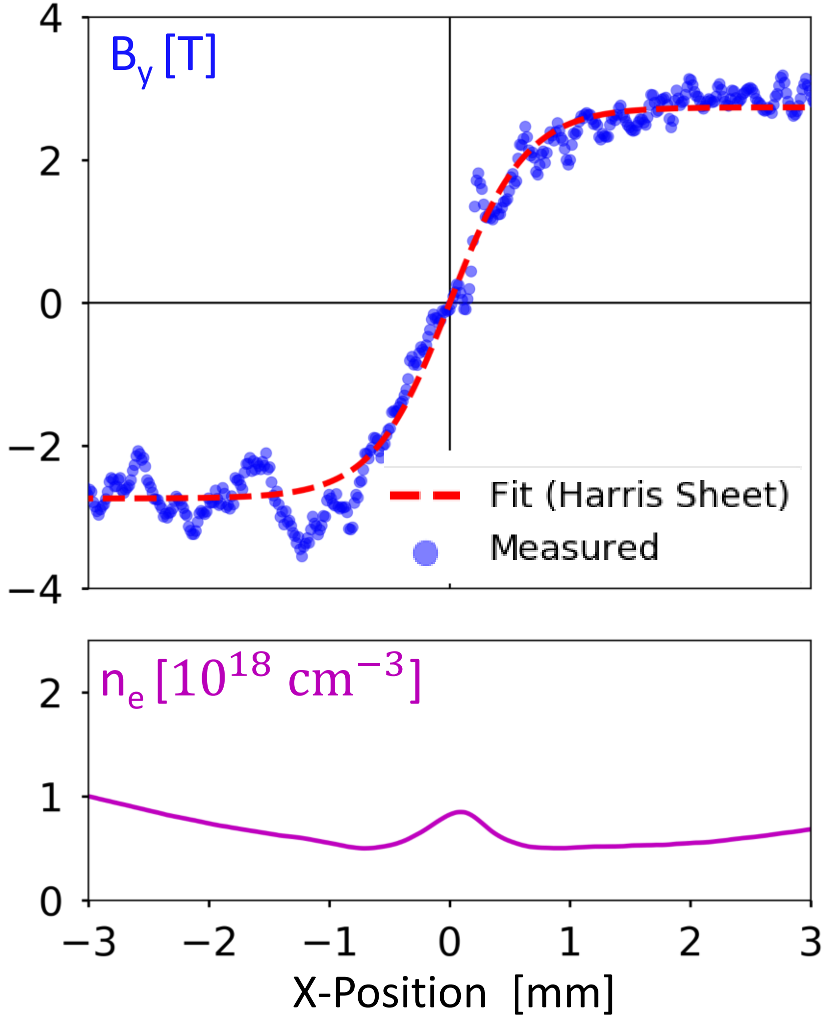

Temperature and Flow Velocity Measurements

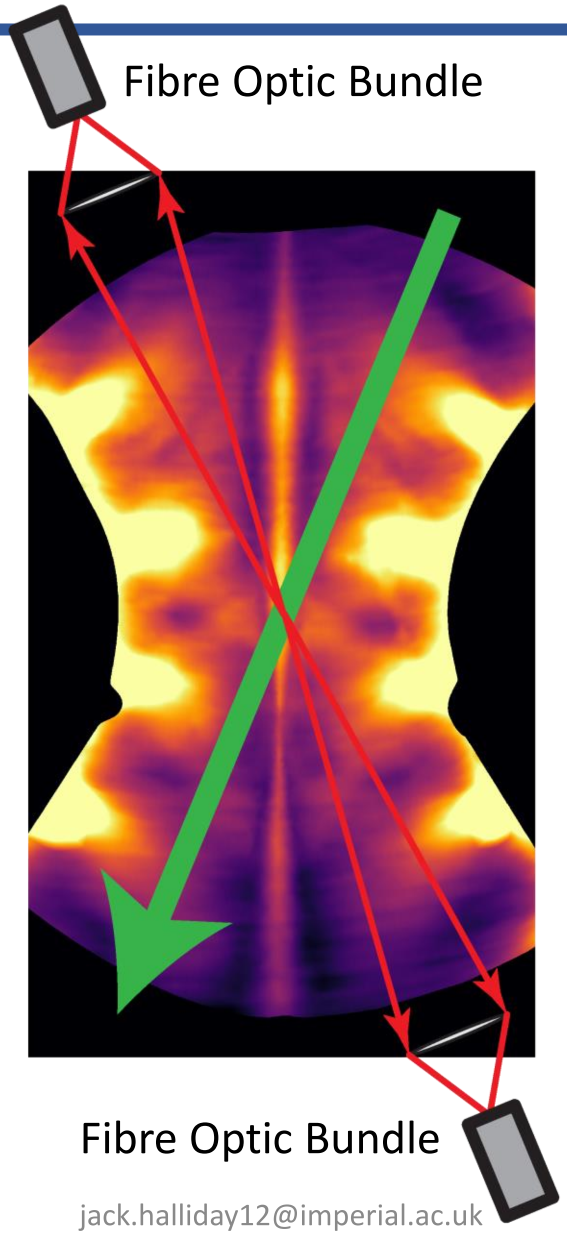

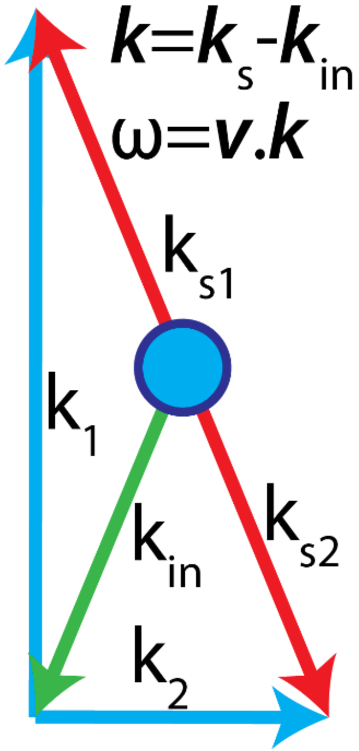

Temperature and Flow Velocity Measurements

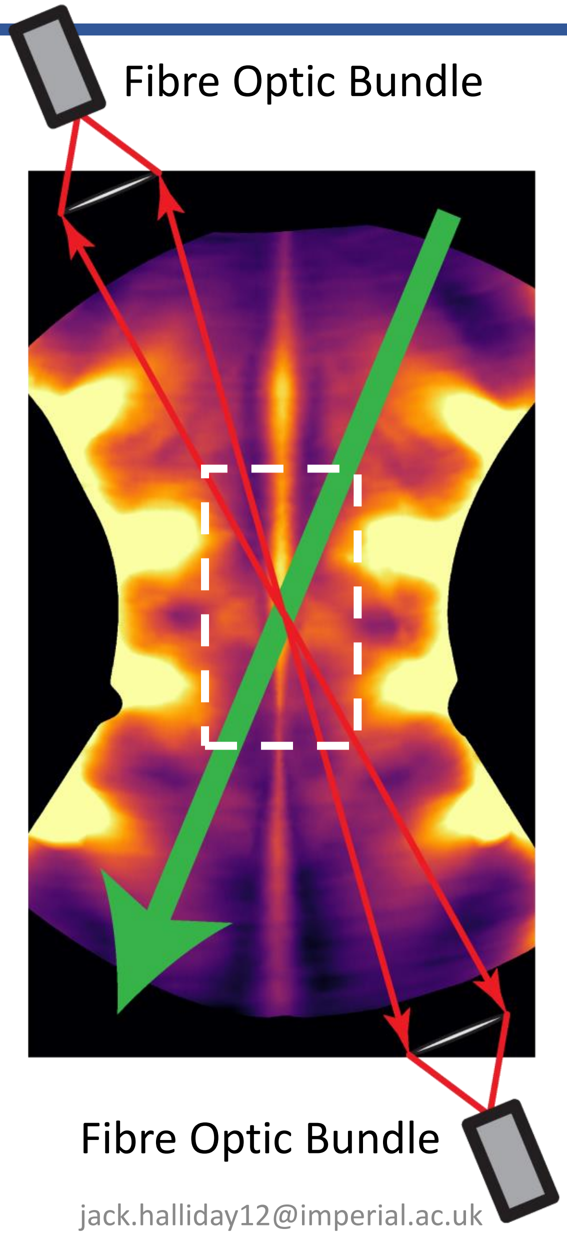

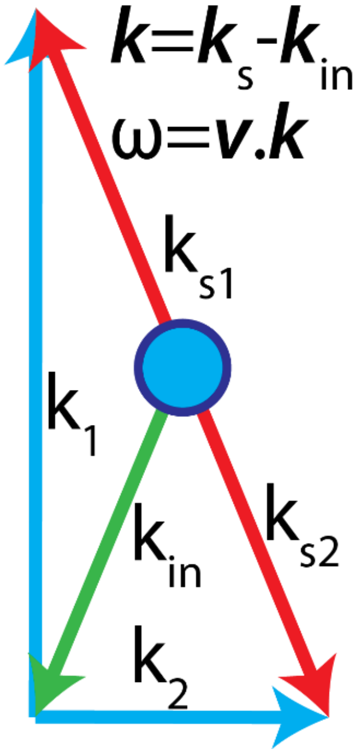

Temperature and Flow Velocity Measurements

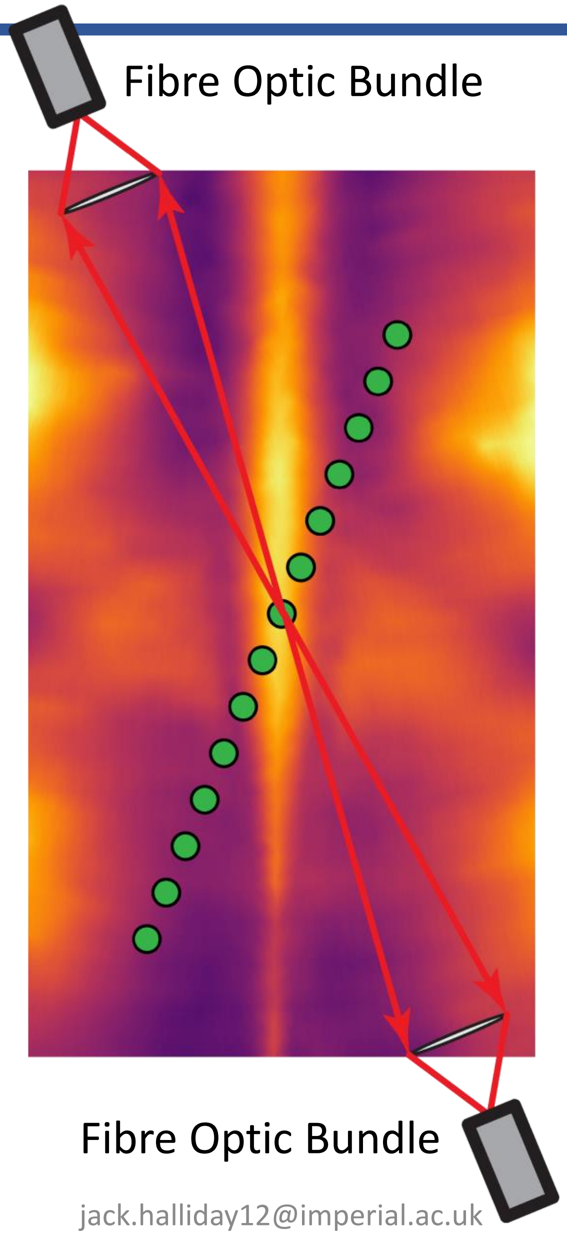

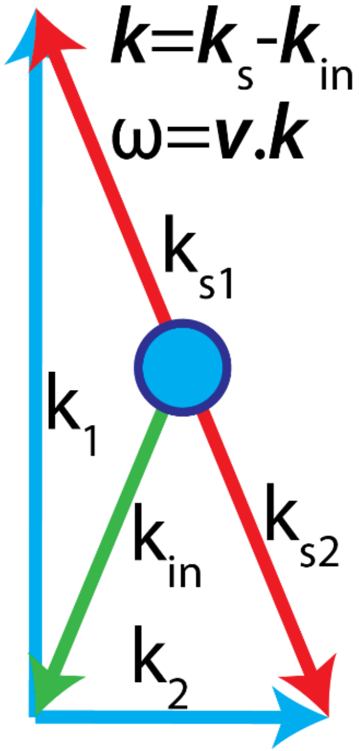

Temperature and Flow Velocity Measurements

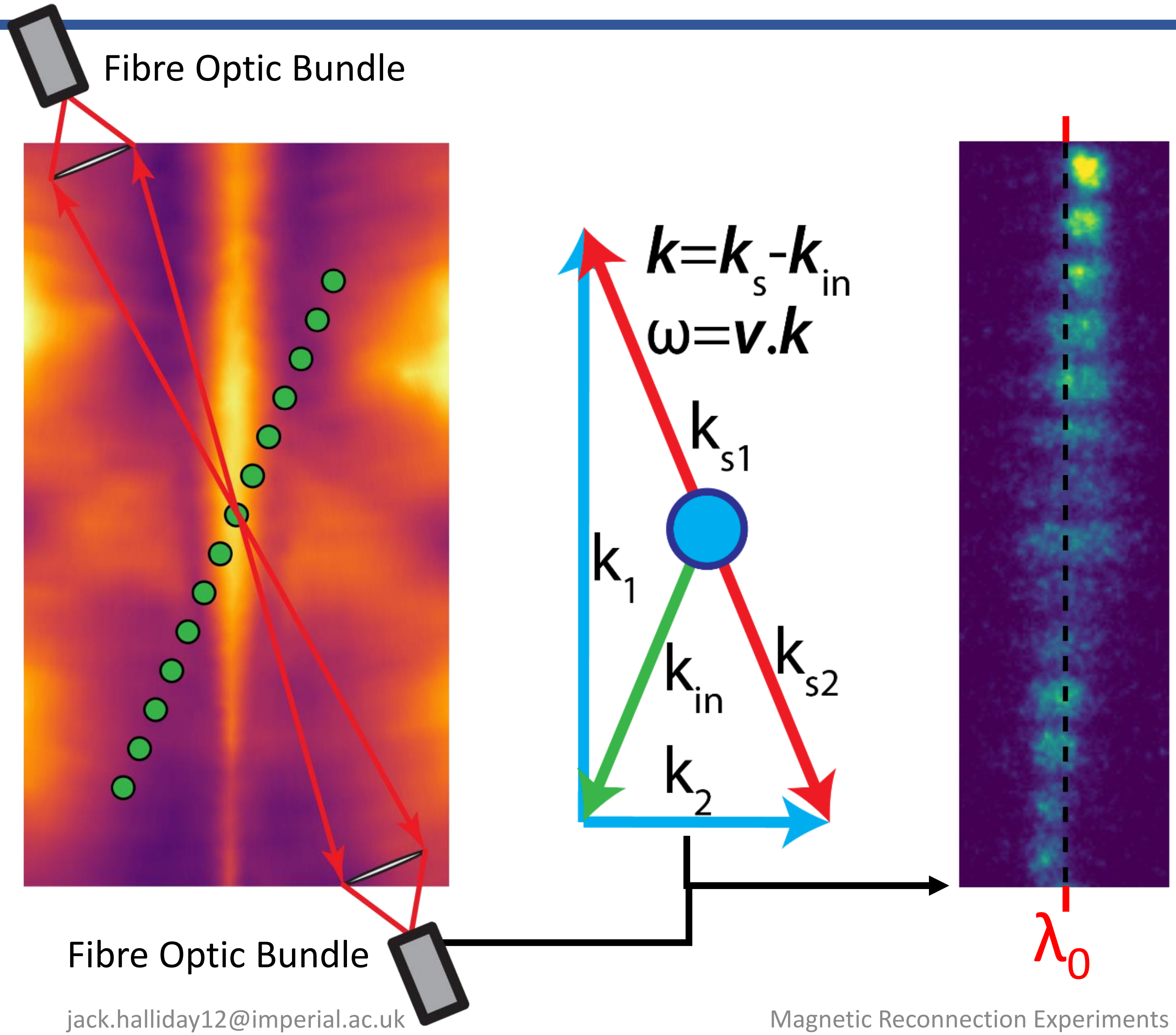

Temperature and Flow Velocity Measurements

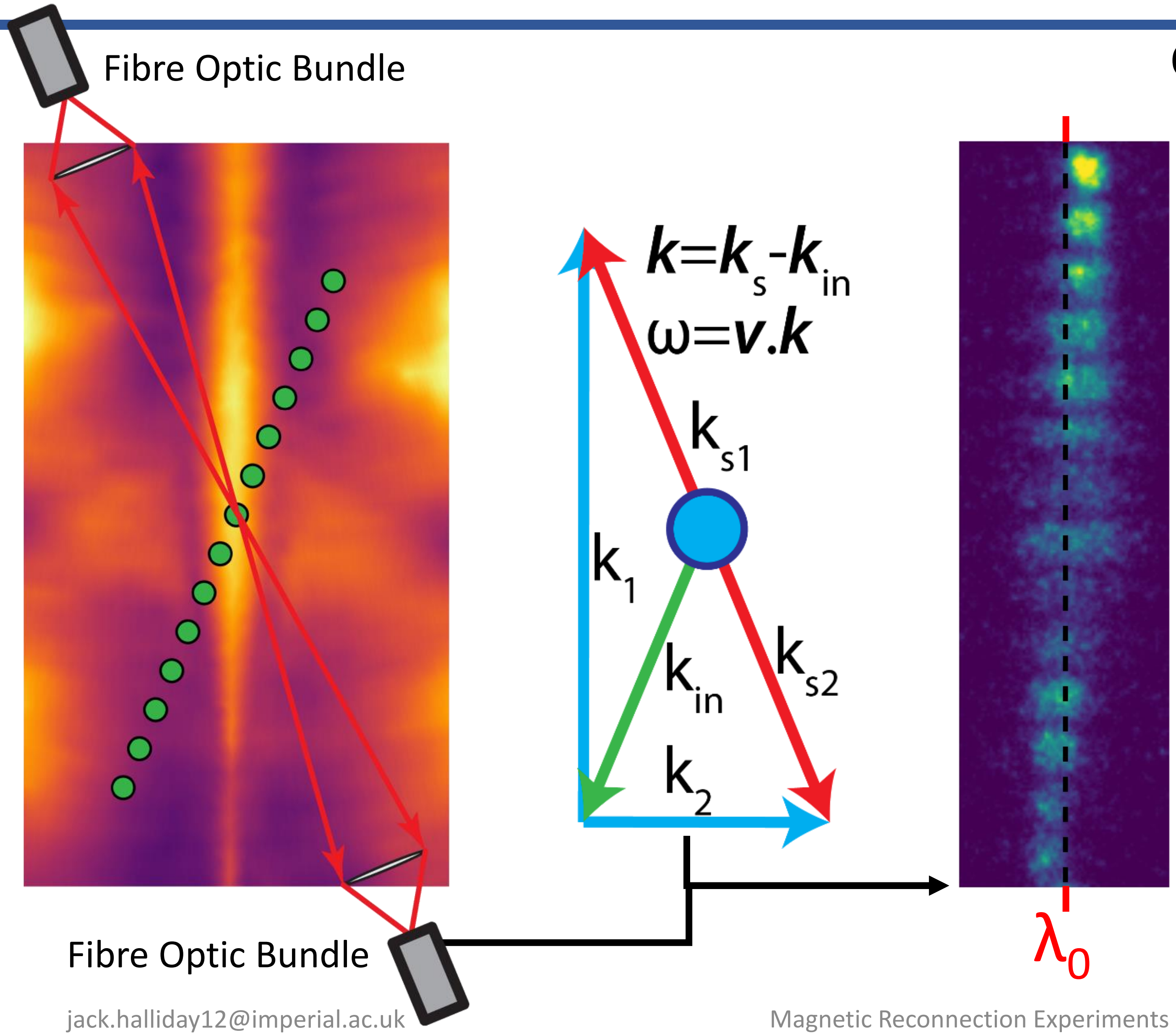

C_s= 30 km/s, V_A= 70 km/s

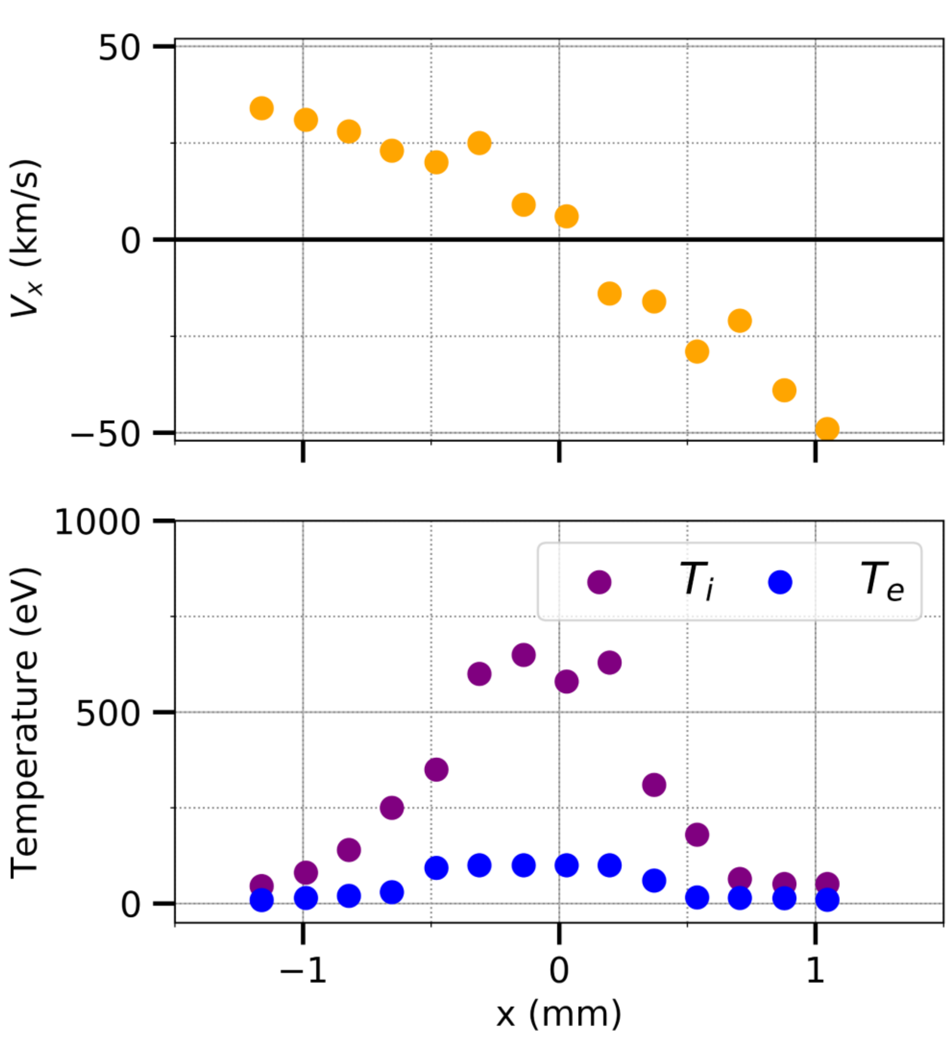

Temperature and Flow Velocity Measurements

C_s= 30 km/s, V_A= 70 km/s

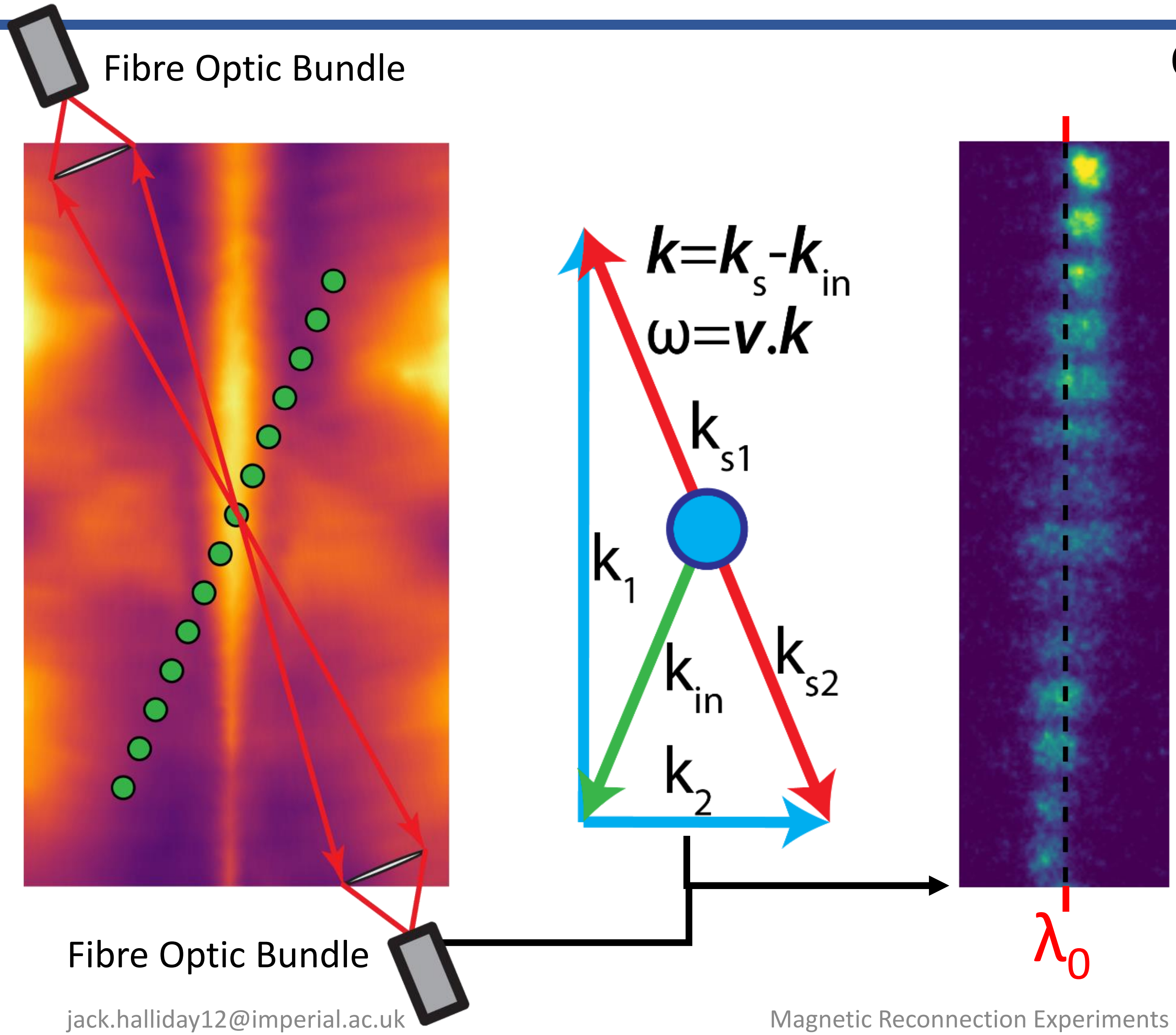

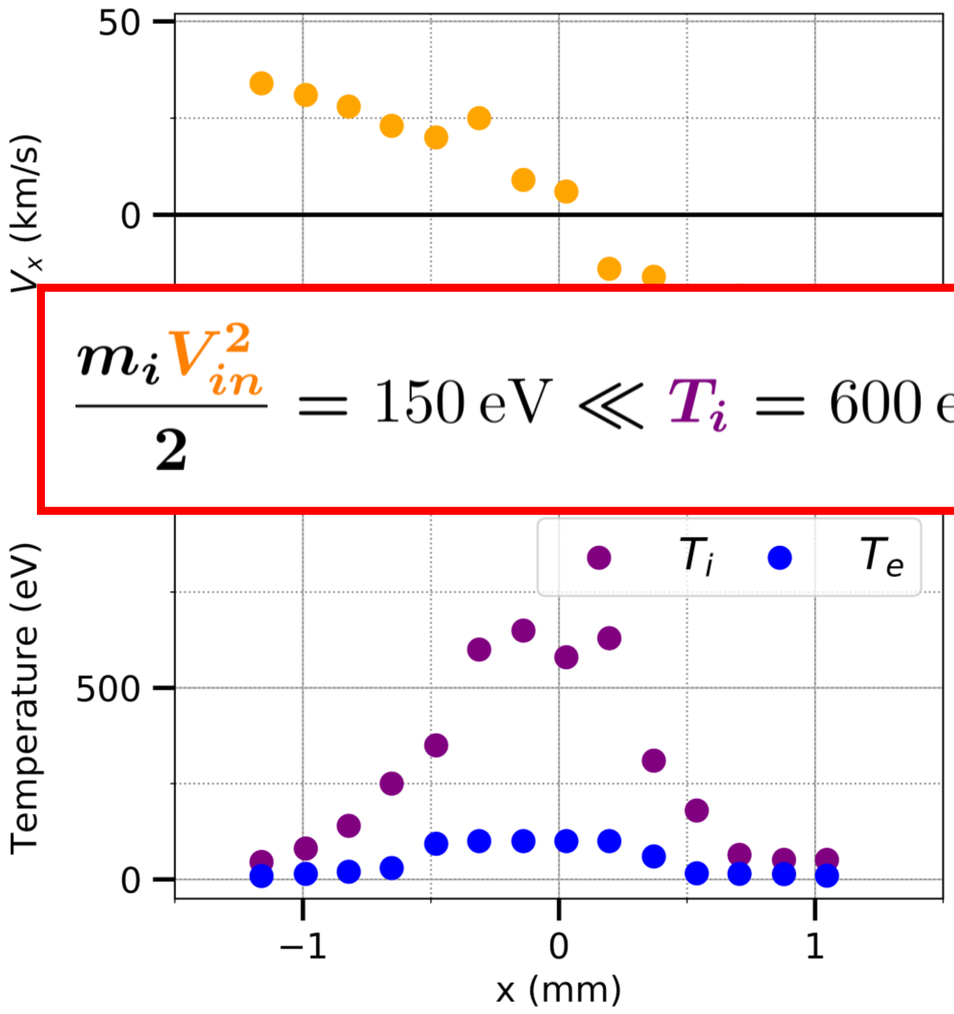

$$\frac{m_i V_{in}^2}{2} = 150\,\text{eV} \ll T_i = 600\,\text{eV}$$

Power Balance in the Reconnection Layer

$$V_{in}Lh\left(E_{mag} + E_{kin} + E_{th,i} + E_{th,e}\right) \approx V_{out}\delta h\left(E_{kin} + E_{th,i} + E_{th,e}\right)$$

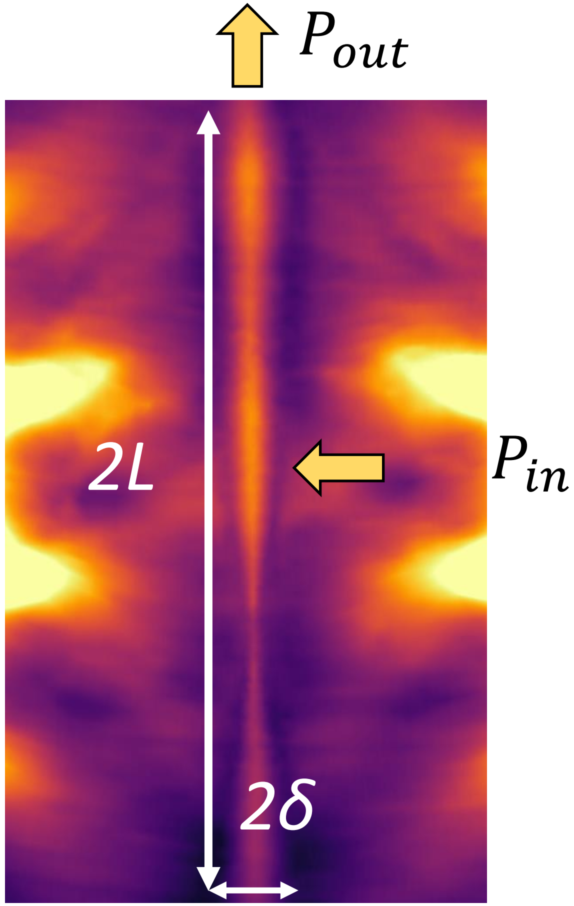

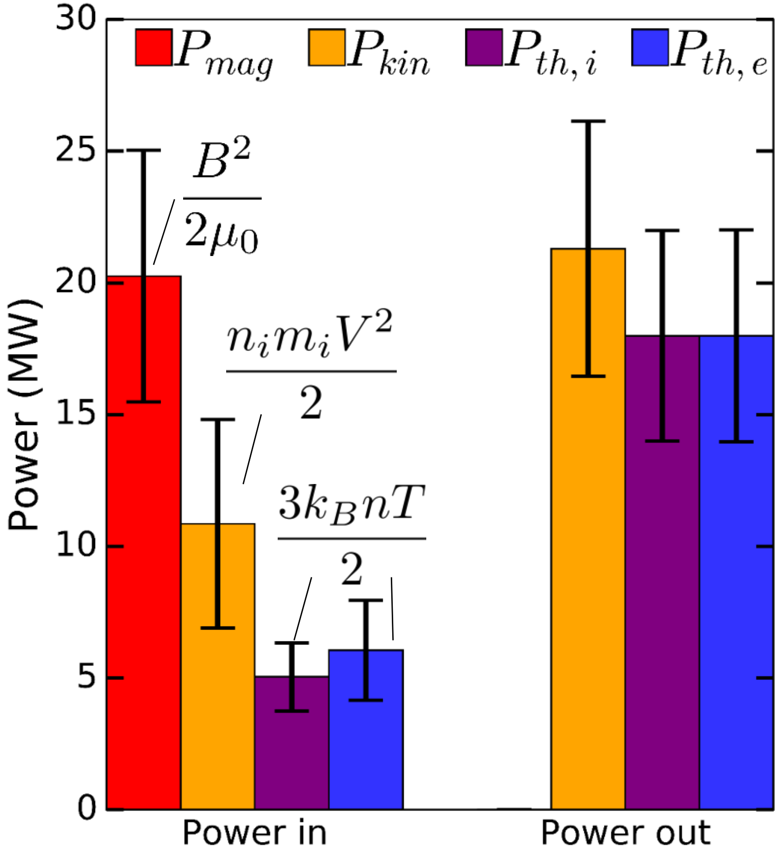

Power Balance in the Reconnection Layer

$$V_{in}Lh(E_{mag} + E_{kin} + E_{th,i} + E_{th,e}) \approx V_{out}\delta h(E_{kin} + E_{th,i} + E_{th,e})$$

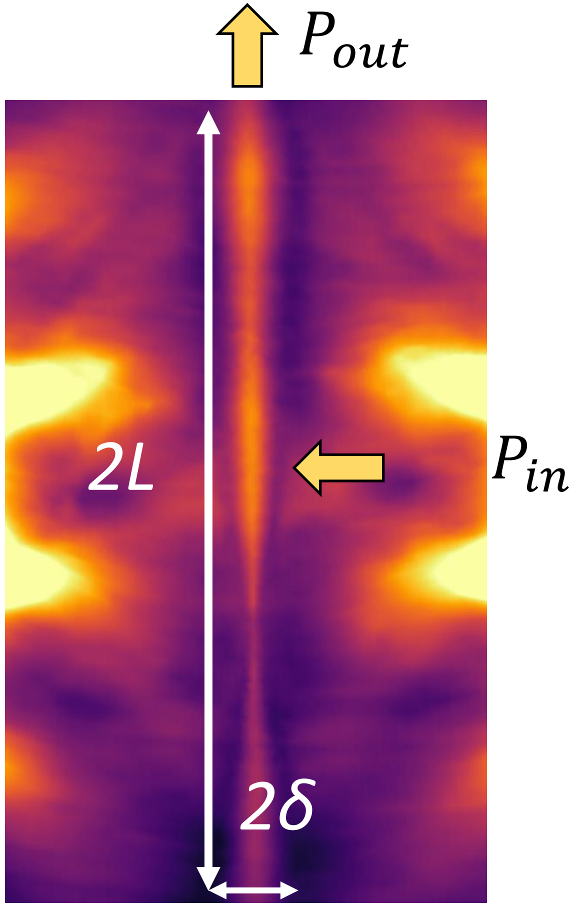

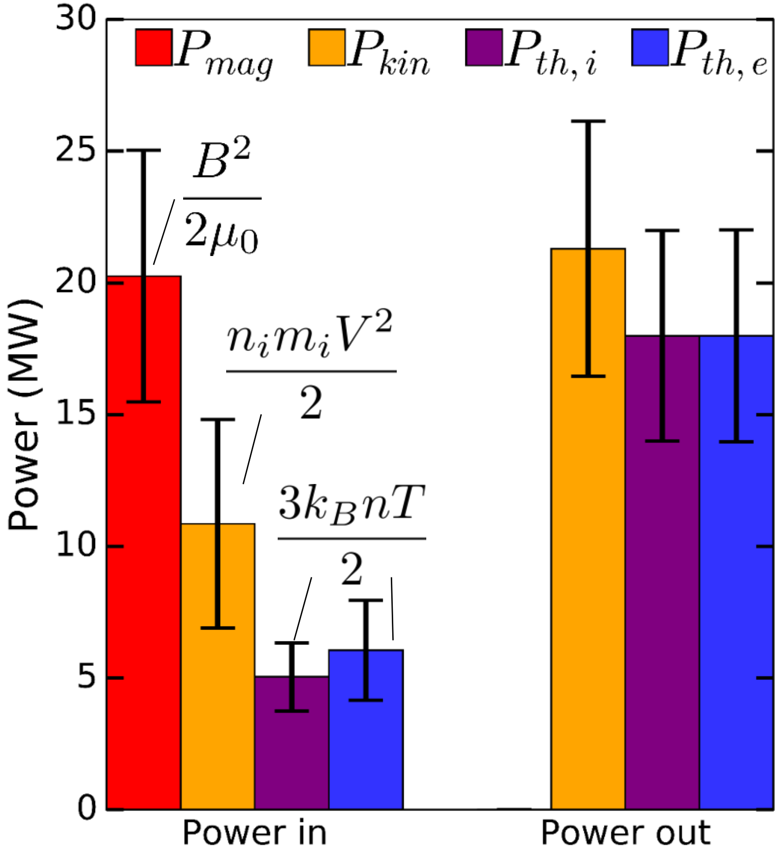

Classical heating is too slow:

$\tau_{exp} \approx 50$ ns

$\tau_{visc} \approx 800$ ns

$\tau_{res} \approx 350$ ns

$\tau_{exp} \ll \tau_{visc}, \tau_{res}$

Overview

- Description of experimental setup
- Diagnostic techniques (Interferometry, Faraday Rotation Thomson Scattering)
- Demonstration of power balance
- Plasmoid unstable reconnection

Plasmoid Unstable Magnetic Reconnection

Aluminium Plasma ($S \sim 10$)

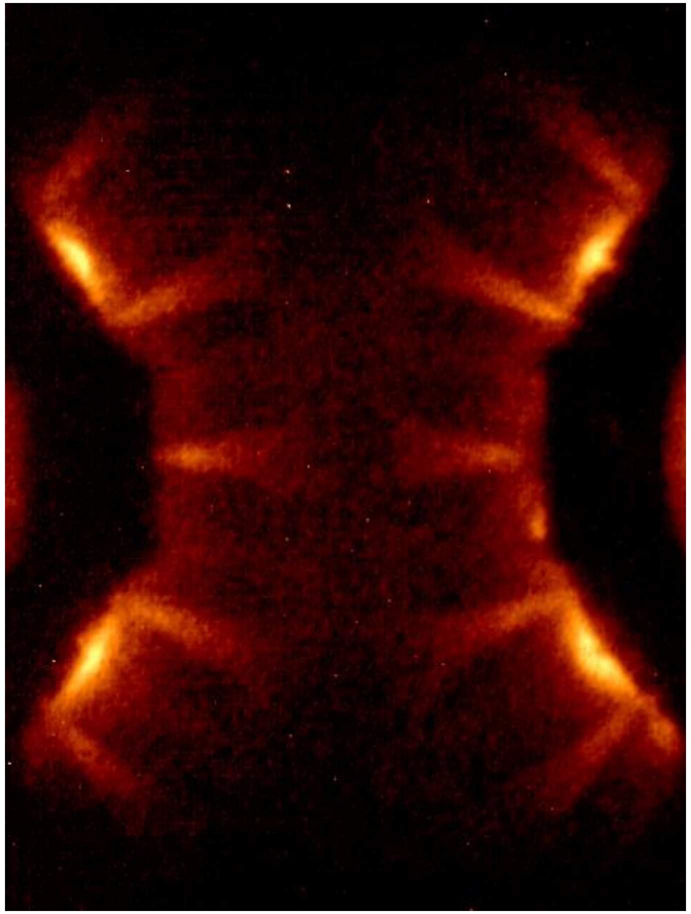

Carbon Plasma ($S \sim 100$)

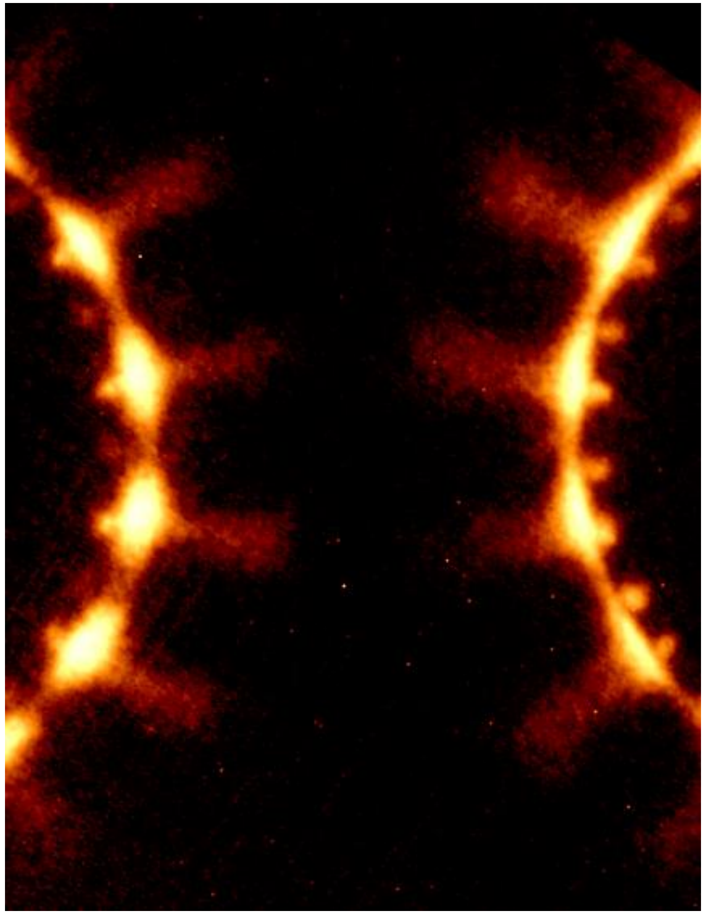

Semi-Collisional Plasmoid Instability

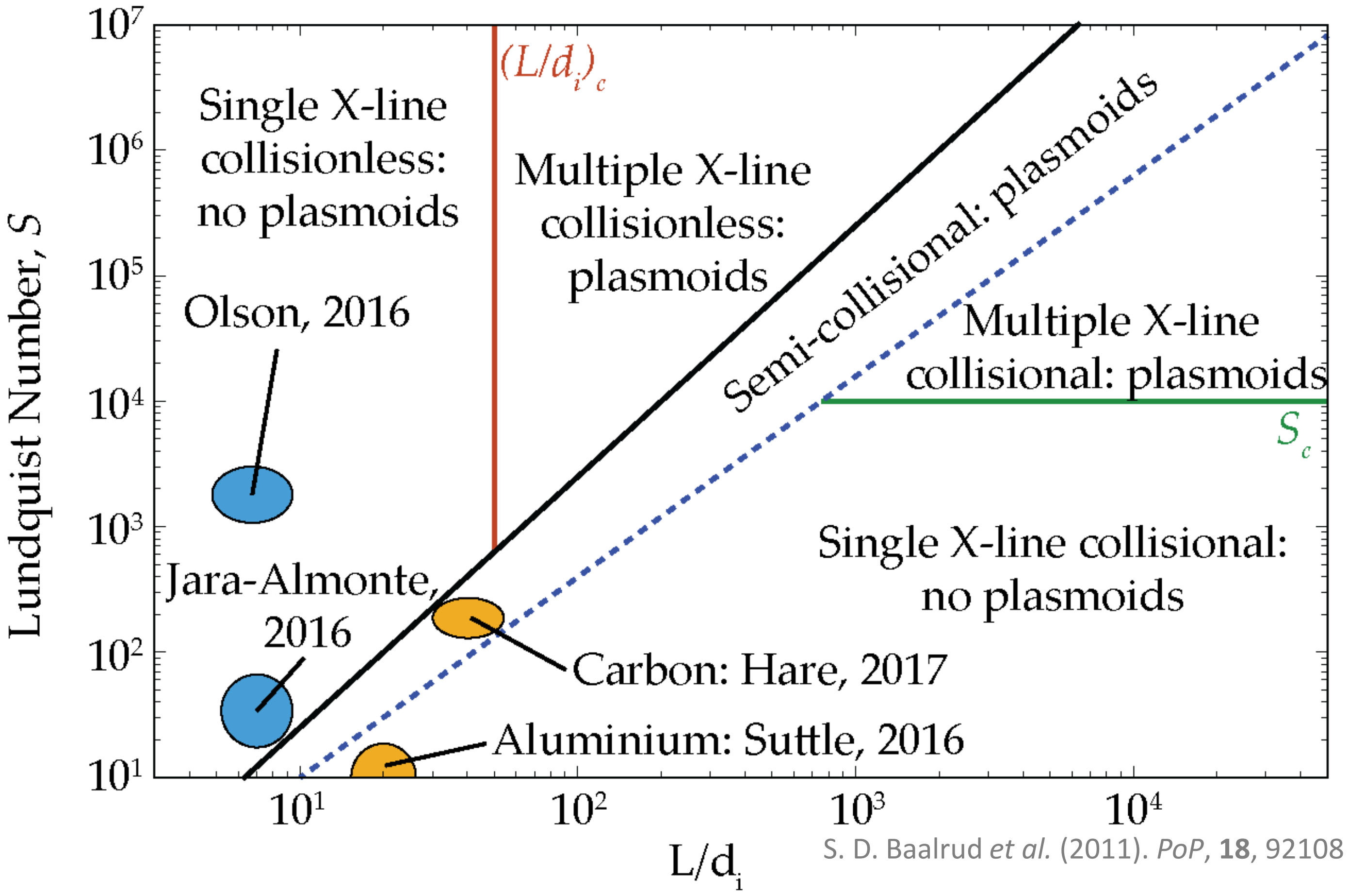

S. D. Baalrud *et al.* (2011). *PoP*, **18**, 92108

$$S = \frac{\mu_0 L V_A}{\eta_{Sp}} \quad \text{[Lundquist number]}$$

In-Situ Measurements of Plasmoid Field Structure

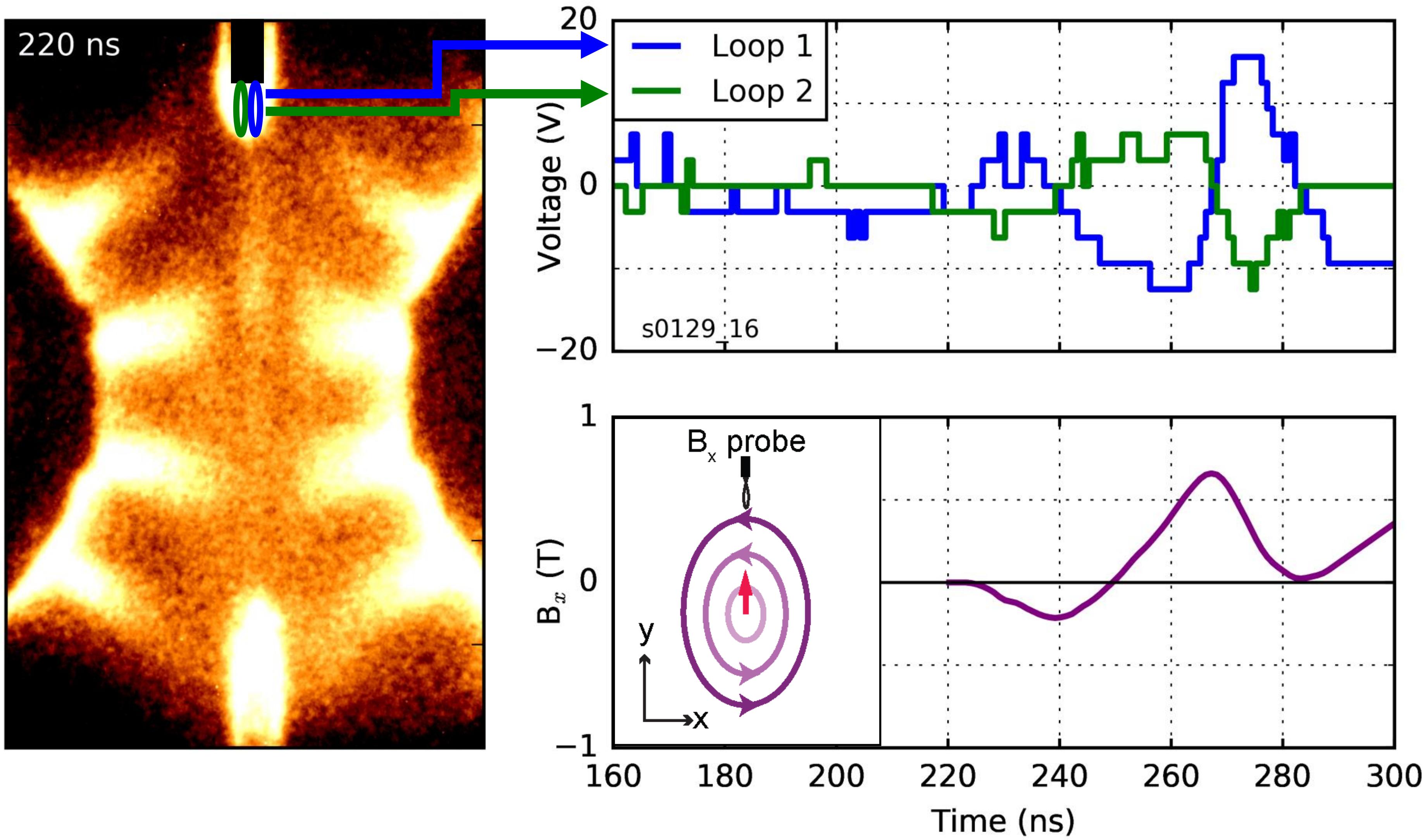

In-Situ Measurements of Plasmoid Field Structure

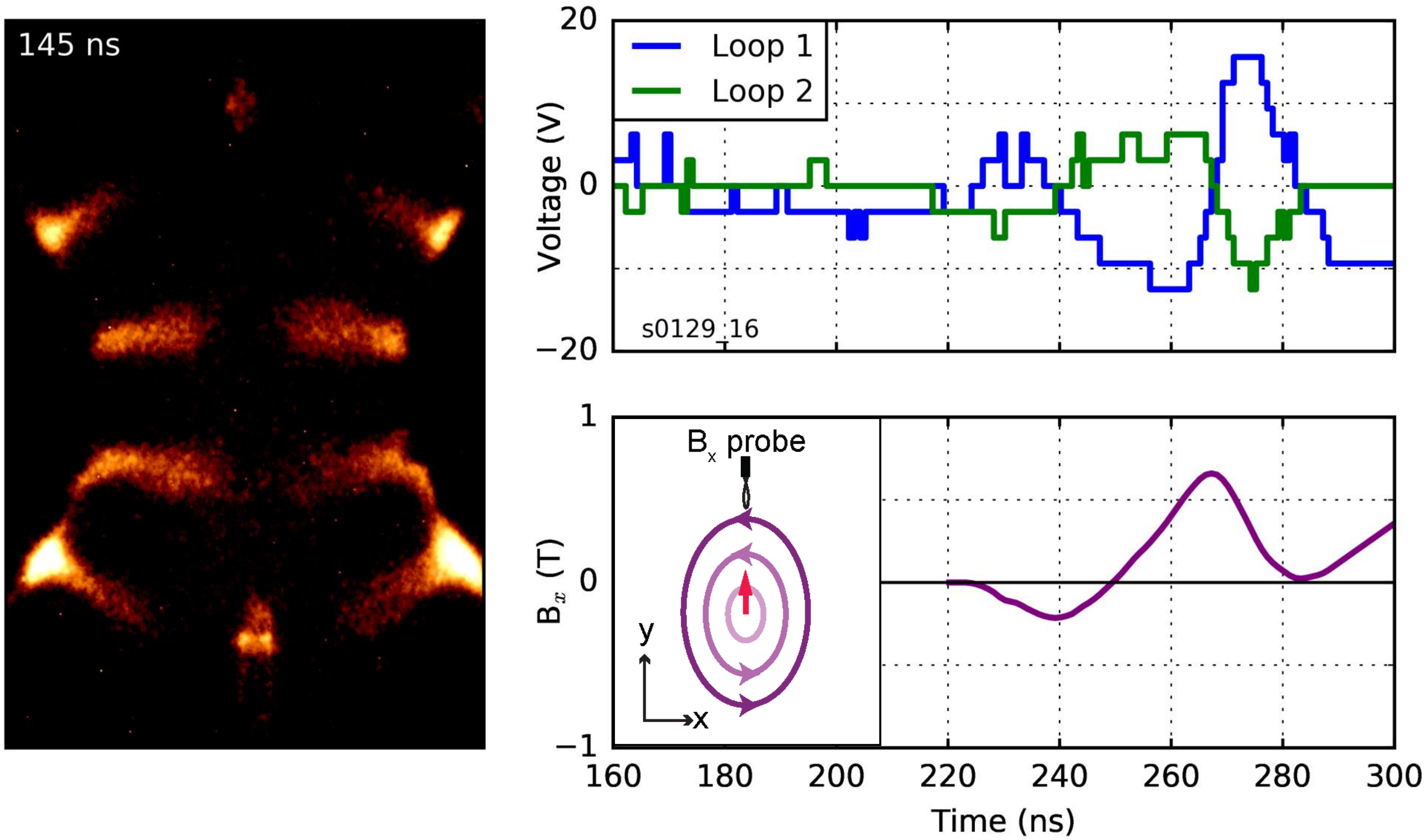

Conclusions

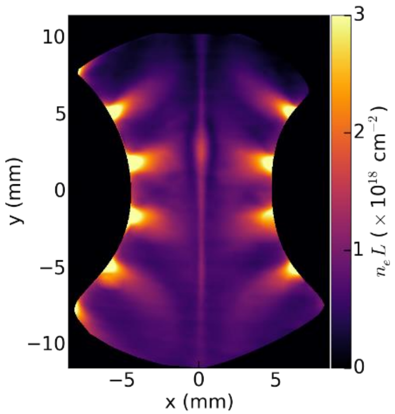

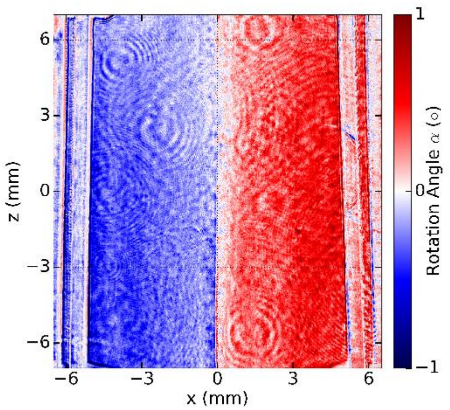

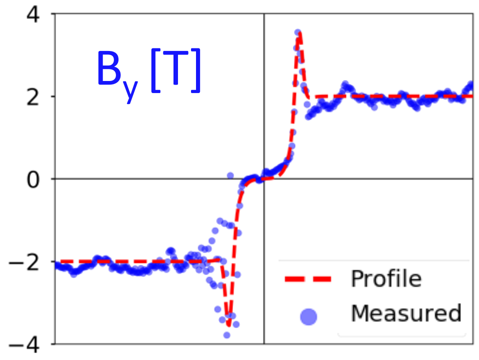

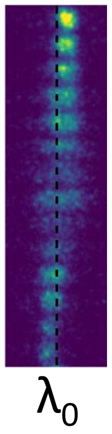

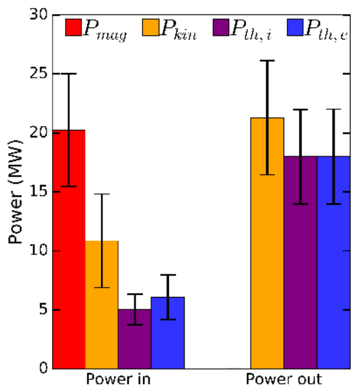

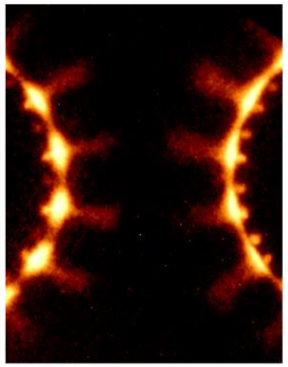

- Versatile driven reconnection platform ($M_A \sim 0.7$ or 2)
- Good power balance between inflows and outflows
- Anomalous heating with $T_e \ll T_i$
- Plasmoids observed, consistent with semi-collisional regime

L. G. Suttle *et al.* – PRL 2016; PoP 2018

J. D. Hare *et al.* – PRL 2017; PoP 2017; PoP 2018

Further Work

- Anomalous scattering in the vertical direction (ion-acoustic turbulence)

- Structure along the reconnection layer (temperature / velocity measurements within plasmoids)

- Signatures of plasmoid mergers

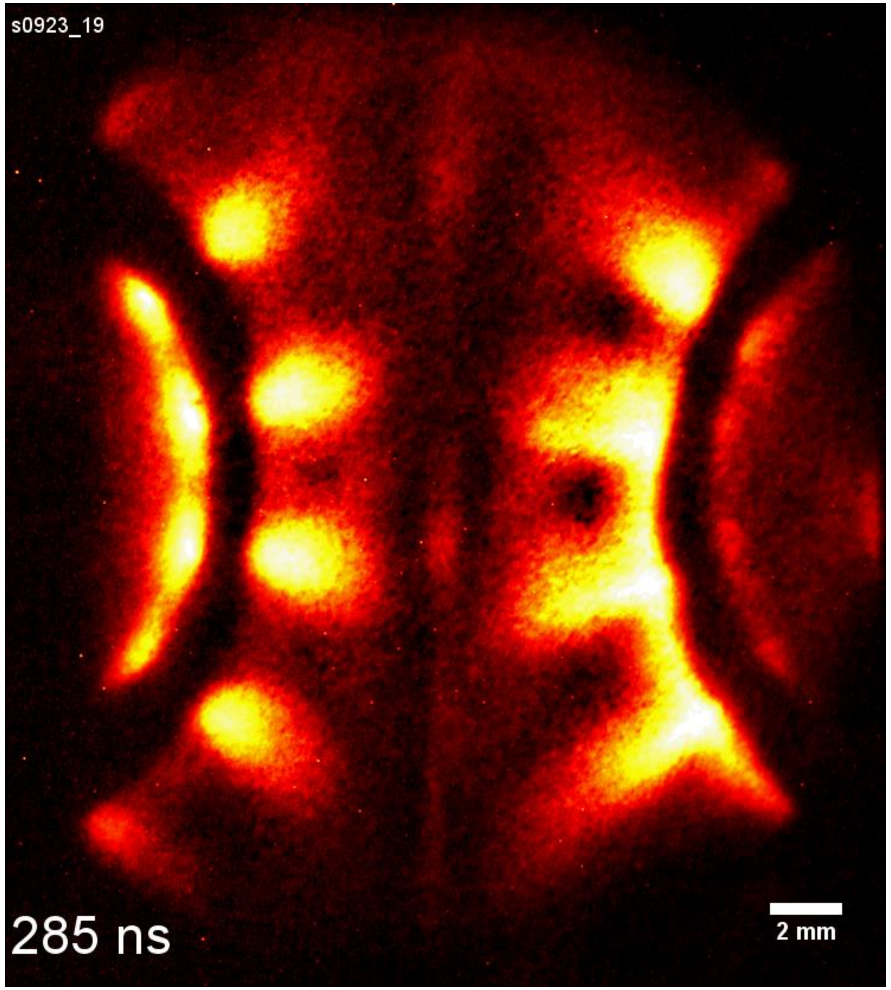

		Aluminium		Carbon	
Parameter		Flow	Layer	Flow	Layer
Electron density (cm^{-3})	n_e	5×10^{17}	$1.4 \rightarrow 2.3 \times 10^{18}$	3×10^{17}	6×10^{17}
Effective charge	$\bar{Z}$	3.5	$7 \rightarrow 5.7$	4	6
Electron temperature (eV)	T_e	15	$40 \rightarrow 30$	15	100
Ion temperature (eV)	T_i	22	$270 \rightarrow 30$	50	600
Magnetic field (T)	B_y	$2 \rightarrow 4$	…	3	…
Layer half-length (mm)	$L = R_C/2$	…	7	…	7
Layer half-thickness (mm)	δ	…	0.3	…	0.6
Ion skin depth (mm)	c/ω_{pi}	0.89	$0.37 \rightarrow 0.33$	0.71	0.41
Ion-ion mean free path (mm)	$\lambda_{i,i}$	6×10^{-4}	3×10^{-3}	4×10^{-2}	3×10^{-3}
Inflow (outflow) velocity (km/s)	V_x (V_y)	50	(100)	50	(130)
Alfvén speed (km/s)	V_A	$22 \rightarrow 35$	…	70	…
Sound speed (km/s)	C_S	16	$44 \rightarrow 27$	30	85
Fast-magnetosonic speed (km/s)	V_{FMS}	$24 \rightarrow 39$	…	75	…
Ion-electron cooling time (ns)	$\tau^E_{e/i}$	50	$40 \rightarrow 20$	30	140
Radiative cooling time (ns)	τ_{rad}	20	$5 \rightarrow 3$	100	600
Thermal beta	β_{th}	1.1	…	0.4	…
Dynamic beta	β_{dyn}	10	…	1	…
Lundquist number	S	…	$11 \rightarrow 7$	…	120
Two-fluid effects	L/d_i	…	$19 \rightarrow 22$	…	18

Plasma Parameters (Carbon Plasma)

Parameter	Inflow	Layer
Electron Density (n_e)	3×10^{17} cm^{-3}	6×10^{17} cm^{-3}
Effective Charge ($\bar{Z}$)	4	6
Electron Temp’ (T_e)	15 eV	100 eV
Ion Temp’ (T_i)	50 eV	600 eV
Layer Half-Length (L)	7 mm	
Layer Half-Width (Δ)	0.6 mm	
Ion skin depth (d_i)	0. 71 mm	0.41 mm
Thermal Electron MFP (λ_{ei}^{th})		9×10^{-2} mm
2 keV Electron MFP ($\lambda_{ei}^{\text{fast}}$)		40 mm
Velocity ($\boldsymbol{v}$)	$50\hat{\boldsymbol{x}}$ km/s	$130\hat{\boldsymbol{y}}$ km/s
Alfven Speed (v_A)	70 km/s	…
Sound Speed (C_S)	30 km/s	85 km/s
Fast MS Speed (v_{fms})	75 km/s	…

Parameter	Inflow	Layer
Alfven Time (τ_A)	100 ns	…
Ion-Elec’ Cooling Time ($\tau_{e\backslash i}^{E}$)	30 ns	140 ns
Radiative Cooling Time (τ_{rad})	100 ns	600 ns
Magnetic Field (B_y)	3 T	…
Reconnecting E Field (E_{Rec})	150 kV/m	
Dreiser E Field (E_D)		2×10^3 kV/m
Thermal Beta (β_{th})	0.4	…
Dynamic Beta (β_{dyn})	1	…
Lundquist Number (S)	100	
Two-Fluid Effects (L/d_i)		18
$\lambda_{ei}^{\text{th}}/L$		1×10^{-2}
$\lambda_{ei}^{\text{fast}}/L$		1
E_{rec}/E_D		4×10^{-2}

Plasmoids in Electron Density Maps

Carbon Plasma

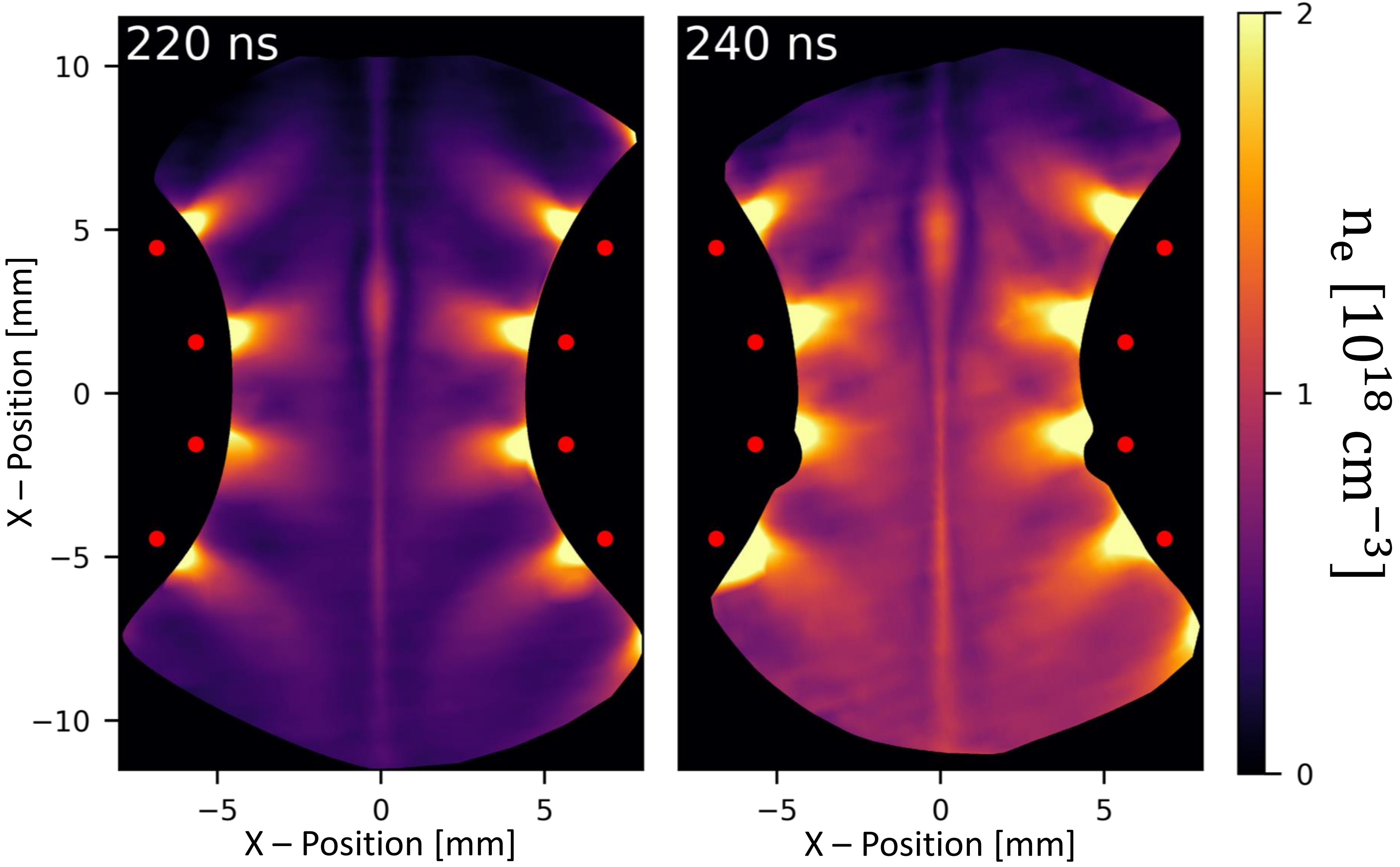

Plasmoids in Electron Density Maps

Carbon Plasma

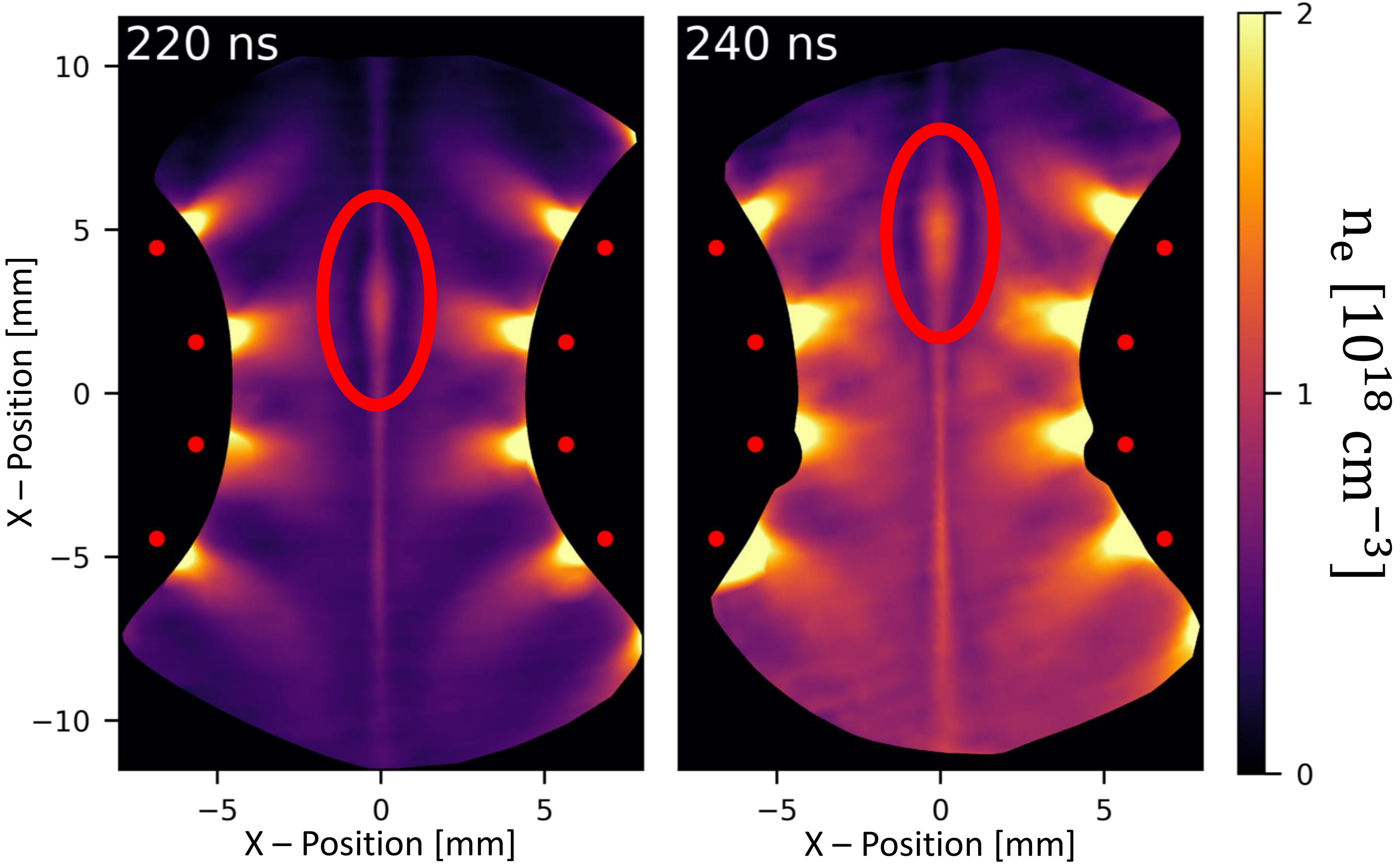

Generalised Sweet Parker Model

Thermal pressure significantly accelerates outflows into vacuum:

$$V_{out} = \sqrt{V_A^2 + 2C_{i,A}^2} = 140 \pm 4\,\mathrm{km/s},$$

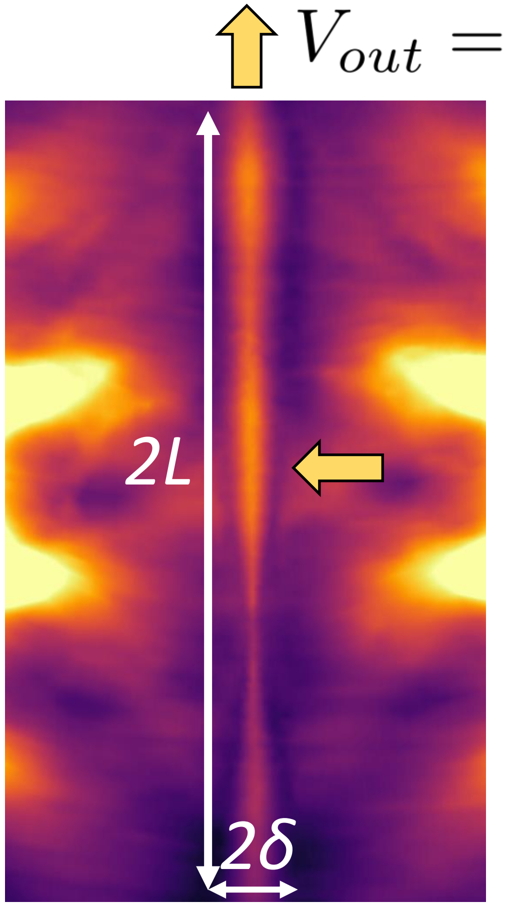

Compressibility and ionisation effects enhance inflow velocity:

$$V_{in} = \frac{\delta}{L}\left(V_{out}\frac{n_2}{n_1} + \frac{L}{n_1}\frac{\partial n_2}{\partial t}\right) = 31 \pm 4\,\mathrm{km/s}$$

$n_{1/2}$: ion density outside/inside layer

H. Ji, M. Yamada *et al.* (1999). *POP*, ***6*** (5), 1743

Neglect Reconnected Magnetic Field

- Sweet-Parker model predicts:

$$B_x = \frac{B_y}{\sqrt{S}}$$

- Magnetic energy in outflow small:

$$\frac{B_x^2}{2\mu_0} = \frac{1}{S}\frac{B_y^2}{2\mu_0} \approx 0.01\frac{B_y^2}{2\mu_0}$$

Anomalous Heating of Electrons

- No energy exchange with ions
- No radiative cooling
- Solve:
- Spitzer resistivity too slow

$$\tau_{E\,e,i} \approx 300\,\mathrm{ns}$$

$$\tau_{rad} \approx 600\,\mathrm{ns}$$

$$\frac{3}{2}\frac{\partial n_e T_e}{\partial t} = \eta_{Sp} j^2$$

$$\tau_{res} \approx 350\,\mathrm{ns}$$

Anomalous Heating of Ions

- No energy exchange with electrons $\tau_{E\,e,i} \approx 300\,\mathrm{ns}$
- Solve:

$$\frac{3}{2} n_i k_B \frac{dT_i}{dt} \approx 0.96\, n_i k_B T_i\ \tau_i \left(\frac{\partial V_y}{\partial x}\right)^2$$

- Classical viscosity too slow $\tau_{visc} \approx 800\,\mathrm{ns}$